



Japan Society of Civil Engineers



## THE BİNGÖL EARTHQUAKE OF MAY 1, 2003

- TITLE
- 1 INTRODUCTION
  - 2 GEOGRAPHY
  - 3 GEOLOGY
  - 4 HYDROGEOLOGY
  - 5 TECTONICS
  - 6 SEISMICITY
  - 7 CHARACTERISTICS OF THE EARTHQUAKE, STRONG GROUND MOTION AND FAULTING
  - 8 GEOTECHNICAL ASPECTS OF THE EARTHQUAKE
  - 9 LIFELINES
  - 10 TRANSPORTATION FACILITIES
  - 11 INDUSTRIAL AND STORAGE FACILITIES.
  - 12 HYDRAULIC STRUCTURE
  - 13 DAMAGE TO STRUCTURES
  - 14 CONCLUSIONS
- ACKNOWLEDGEMENTS
- REFERENCES

**Investigated and Prepared by**

**Ö. Aydan**

**Tokai University, Department of Marine Civil Engineering  
Shimizu-Orido, 3-20-1, Shizuoka, Japan**

**R. Ulusay**

**Hacettepe University, Department of Geological Engineering  
Beytepe, Ankara, Turkey**

**M. Miyajima**

**Kanazawa University, Department of Civil Engineering  
Kanazawa, Japan**

July 2003

Copyrights (C) 2003 JSCE. All Rights Reserved.

# **THE BİNGÖL EARTHQUAKE OF MAY 1, 2003**



**Ö. Aydan**

**Tokai University, Department of Marine Civil Engineering  
Shimizu-Orido, 3-20-1, Shizuoka, Japan**

**R. Ulusay**

**Hacettepe University, Department of Geological Engineering  
Beytepe, Ankara, Turkey**

**M. Miyajima**

**Kanazawa University, Department of Civil Engineering  
Kanazawa, Japan**

**July 2002**

## 1 INTRODUCTION

An earthquake with a magnitude of 6.4 (M<sub>w</sub>) occurred on May 1, 2003 in Bingöl province of the East Anatolian Region of Turkey. This earthquake was officially called *2003 Bingöl Earthquake* and felt at neighboring cities. This province was also hit by an earthquake, which occurred in 1971 and caused heavy damages and loss of life particularly in Bingöl. The Kandilli Observatory and Earthquake Research Institute (KOERI, 2003) of Boğaziçi University estimated that the earthquake centered at 39.01 N and 40.49 E, which places the epicenter about 15 km NW of Bingöl city.

According to official announcements the earthquake caused the loss of 176 lives and injured about 520 people. About 362 buildings collapsed and/or to heavily damaged, and 3026 buildings were moderately - to - lightly damaged in Bingöl city center. The number of collapsed or heavily damaged buildings in the whole earthquake affected region is announced as 625 and a total of 3650 were subjected to damage of different degrees.

Landslides and a large lateral spreading triggered by the earthquake also occurred. Landslides were mainly in the mode of earth flows in highly weathered volcanics and rock falls from steep slopes, which were observed at rural areas. Focal plane solutions from several institutes indicate two possible strike-slip faults striking NW-SE and NE-SW. On the contrary to those observed in the devastating 1999 Kocaeli and Düzce earthquakes of Turkey, evident surface ruptures could not be clearly traced on the land in this earthquake. However, very short and thin cracks observed at the epicentral location are considered to be associated with the possible causative fault.

Most of the buildings in Bingöl are typically multi-story commercial/residential reinforced concrete structures. A large percentage of collapsed and/or severely damaged buildings were generally in 3 to 6 story range. The damage seems to be resulted mainly from poor quality construction and inappropriate construction materials. The minarets of mosques exhibited a very good performance, except a few in Bingöl city and Karakoçan town.

Although the bridges exhibited a good performance, there were some damage to a few highway bridges near Bingöl. Dams in the earthquake-affected region were almost non-

damaged. In spite of relative small displacements of the transformers and some slight damage to the telecommunication building in Bingöl, no important problems associated with electricity and communication facilities were observed in the region.

The investigation team of Japan Society of Civil Engineers (JSCE) consisting of two members from Japan and one investigator from Turkey conducted a field investigation in the earthquake region for five days from May 30 to June 3, 2003 (Figure 1.1). During the field investigation; team members visited strong motion observation station located in Bingöl city center, carried out some observations and took some measurements on the collapsed and damaged structures and lifelines. In addition, local site conditions were also assessed with the aid of data from recently drilled geotechnical boreholes and trial pits at some collapsed and heavily damaged buildings in Bingöl. This report outlines the findings of the investigation undertaken by the JSCE team on various aspects of the earthquake in Bingöl province.



Figure 1.1: Investigation Route of the JSCE team

## 2 GEOGRAPHY

The province where the earthquake of May 1, 2003 occurred, is located at the Upper Murat Section of the East Anatolia region of Turkey (Figures 2.1, 2.2 & 2.3). There are closely or widely spaced ridges, cut-through valleys, and some plains. Bingöl city is founded on flat terraces surrounded by high mountains from its north, northeast and west. Except Bingöl Plain (Ova) with an extent of 80 km<sup>2</sup> and Murat River valley at the southeast of Bingöl city, the province is generally mountainous. The elevations of the mountains reach up to 3000 m and the elevation of the Bingöl city center is about 1125 m.

The amount and regime of precipitation varies considerably. Winters are long and severe, and the ground is covered by snow between December and April. The summers pass dry. Because of little precipitation in the lowlands, the vegetation cover tends to have steppe characteristics. Mountains are generally devoid of vegetation, however, local woodlands consisting mainly of oak trees may be observed. In the mountainous areas, the settlements are rather scattered. Because of water-supply problem, the villages are usually set up in rows along valleys.



Figure 2.1: Location of Bingöl Province



Figure 2.2: Physico-geographical features of Bingöl Province and its close vicinity

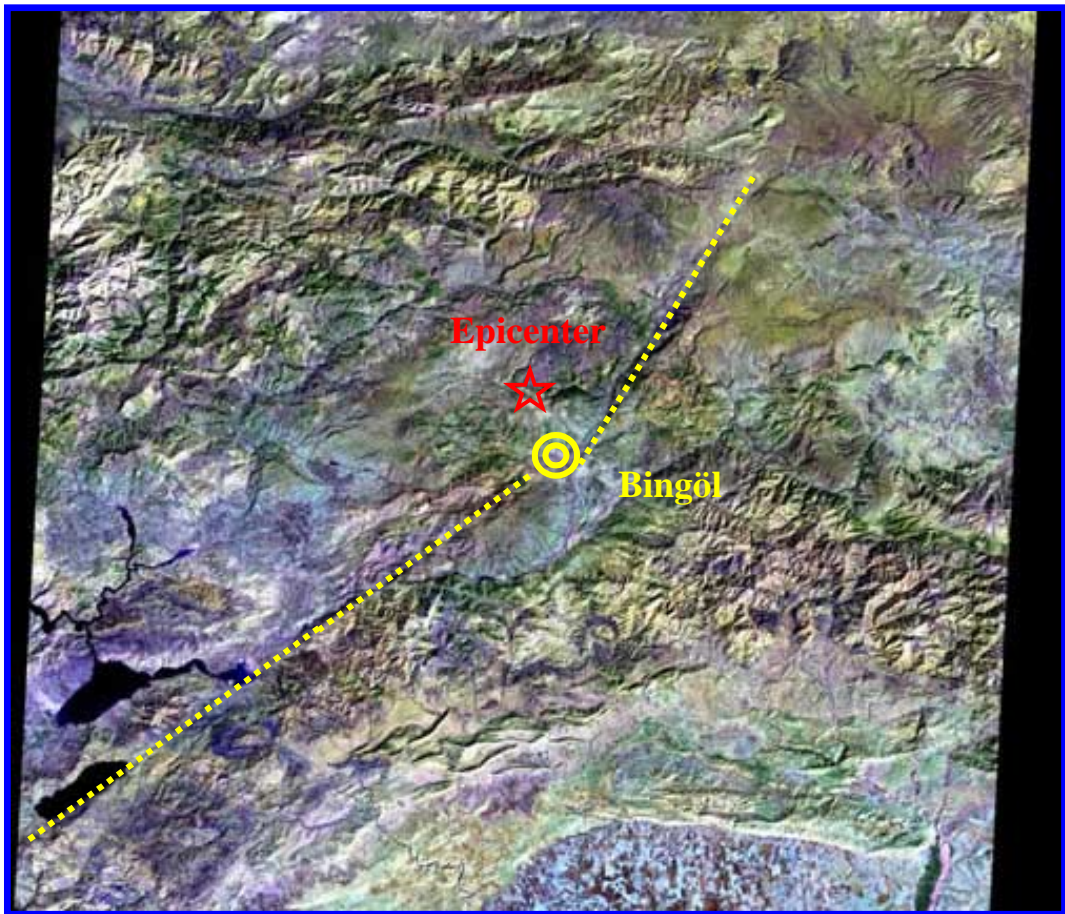


Figure 2.3: LANDSAT image of Bingöl Province and its close vicinity

### 3 GEOLOGY

The earthquake affected region is mainly covered by the Upper Oligocene-Lower Miocene aged volcanic rocks as seen from the simplified geological maps (Figures 3.1 and 3.2). (Seymen and Aydın, 1972), which extend along a very large corridor trending E-W. Various metamorphic rocks at the south, and acid intrusions, serpentine, ophiolites and flysch rocks of different ages, Neogene continental deposits and Quaternary-aged old and new alluvial deposits with limited extent are also observed. Basalts and andesites mainly represent these volcanic rocks. Sometimes trachyte and rhyolites are also observed within the volcanics (Altınlı et al., 1963; Seymen and Aydın, 1972). Andesites, which transformed into residual soil place to place due to extensive weathering and/or alteration, appear in brown and red colors (Figure 3.3a). Basalts exhibit pillow and columnar structures, and spheroidal weathering as shown in Figures 3.3 b-c. Mostly tuffs are found interbedded with lava flows, contrasting the latter's dark color with their light color and texture. They are well observed between Sancak town and Kurtuluş village in the epicentral area at the north of Bingöl and have been weathered and/or altered. The tuffaceous grounds exhibit a badland topography with caves and sometimes pillars (Figure 3.3 d).

The Bingöl Plain has been formed by the lateral jointing of the composite alluvial cones , which came down into the basin from the mountains. The Quaternary deposits are only observed in this plain (Figure 3.1) in the earthquake-affected region, and consist of Plio-Quaternary terrace deposits and recent alluvium. Bingöl city center is founded on thick terrace deposits as seen from the detailed geological map of the city and its vicinity given in Figure 3.2. Terrace deposits, which appear between the elevations of 1040-1000m, are clearly observed on terrace slopes and in the trial pits reaching up to 4-5 m depths excavated near some collapsed buildings in Bingöl. They are composed of round and semi-round blocks in different sizes within a stiff clay matrix (Figure 3.4 a). Based on the data from geotechnical boreholes drilled in Bingöl by a private company (Yüksel Proje A.Ş.), silty and sandy levels are also present in this sequence. However, towards southeast of Bingöl, at flat-lying areas (i.e. at Çeltiksuyu), the amount of blocks reduces and sandy clays and silts become dominant. Natural and man-made slopes in the terrace deposits are generally stable even they have been subjected to earthquake shaking (Figure 3.4 b).

As can be seen from Figures 3.1 and 3.3, recent alluvial deposits cover the southern and southeastern parts of Bingöl city and extend to Genç town at south. These deposits have been carried and accumulated mainly by Gayıt and Göynük Brooks. They consist of gravel, sand, silt and clay sized materials in different fractions. They form flat lying areas (Figure 3.4c) and occasionally alluvial cones.



<b>Qy</b> Holocene (recent alluvium)	<b>Cr</b> Metamorphic series (undifferentiated)
<b>Qe</b> Pleistocene (old alluvium)	<b>z</b> Asit intrusives
<b>n</b> Neogene (continental, undifferentiated)	<b>s</b> Serpantine
<b>md</b> Miocene (marine, undifferentiated)	<b>α</b> Andesite, spilite, porphyrite
<b>ef</b> Eocene (flysch)	<b>β</b> Basalt, dolerite
<b>Mof</b> Mesozoic (ophiolitic series)	<b>- - -</b> Probable fault

Figure 3.1: Geology of Bingöl Province (after MTA)

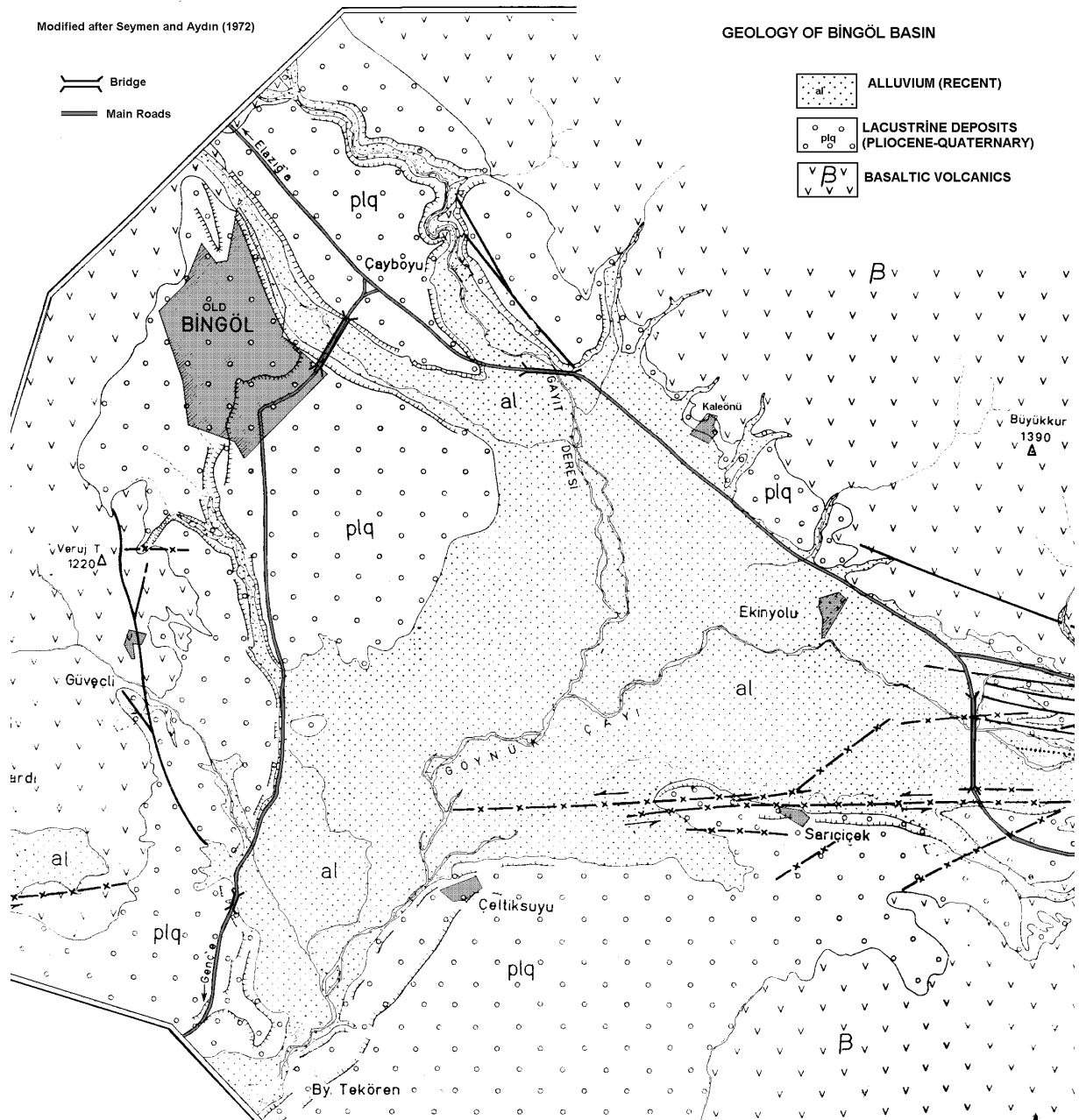


Figure 3.2: Geology of Bingöl (after Seymen and Aydın 1972)

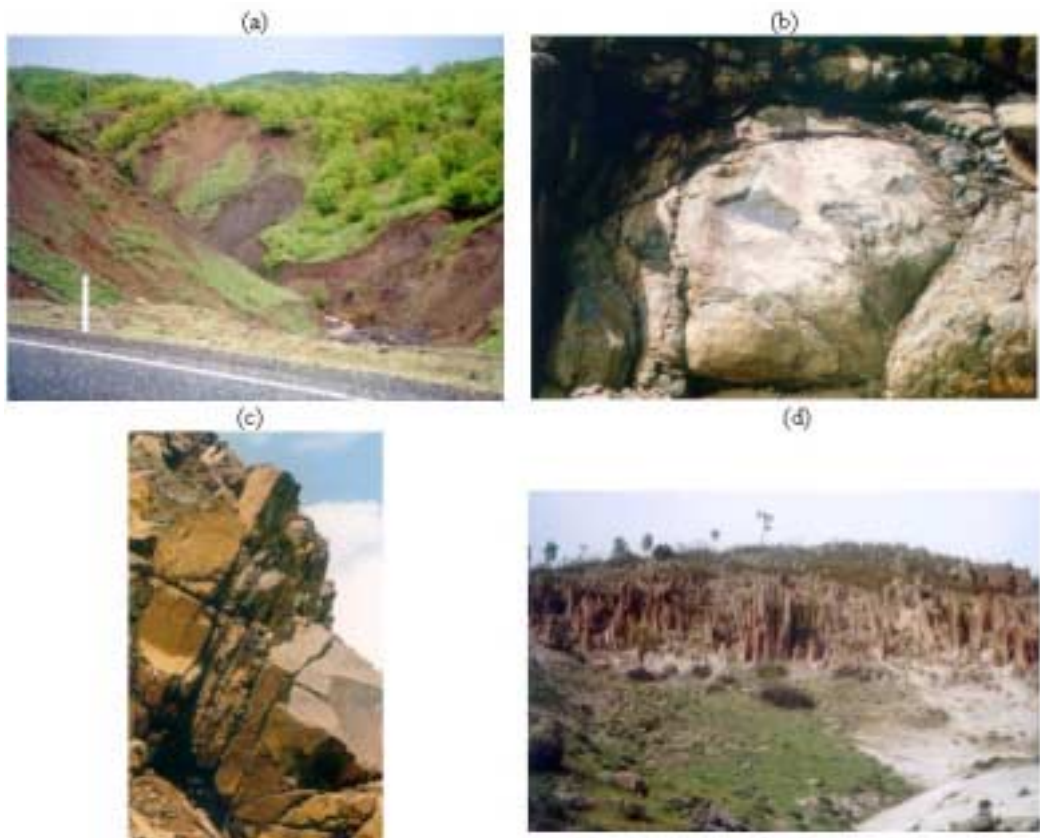


Figure 3.3: Views of rock outcrops

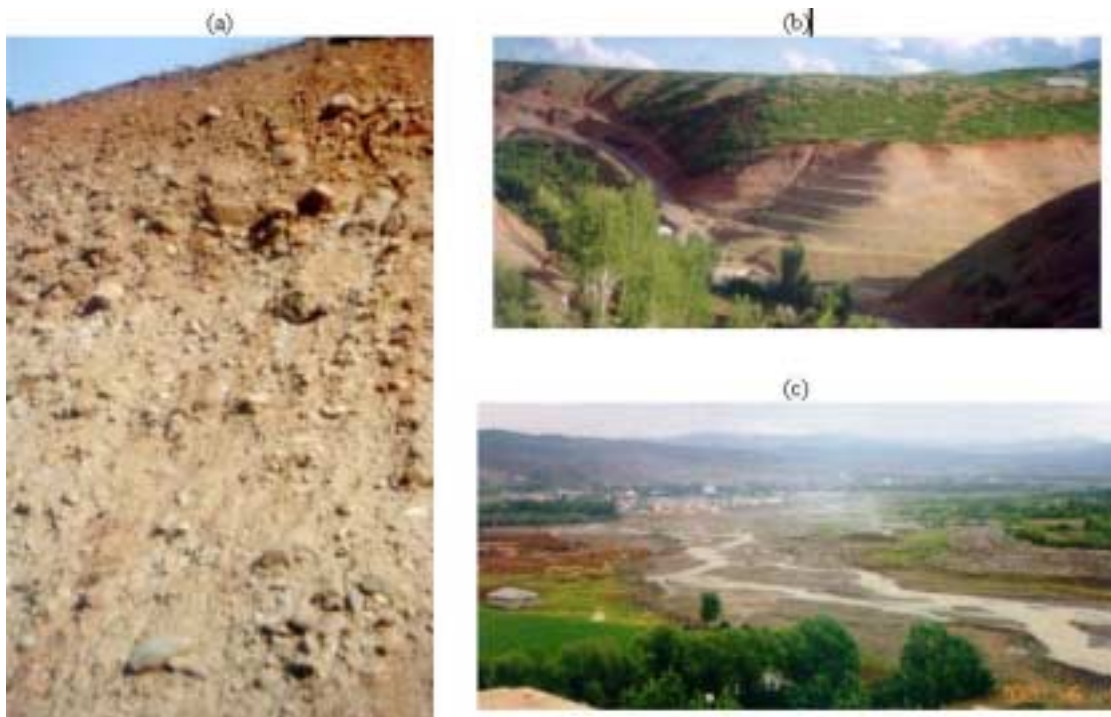


Figure 3.4: Views of soil deposits

#### 4 HYDROGEOLOGY

Murat River is the longest river in Bingöl region. The river cuts across the mountain chain in the north of Muş City through a structural depression with an intensive down-cutting. Göynük Brook follows partly fault lines and flows in NE-SW direction at the east of Bingöl city (Figure 3.2). The Gayt Brook bed divides the terrace deposits underlying Bingöl city by a deep valley extending in E-W direction and joins to Göynük Brook in the east (Figure 4.2). Another stream, which passes between the terraces on which Bingöl located, is the Çapakçur Brook (Figure 4.3).

Although there is no available report on the hydrogeology of the Bingöl Plain, the data from the geotechnical boreholes, which were 15 m deep and drilled in Bingöl city after the recent earthquake, were assessed for the purpose. Except a few boreholes, no groundwater level was encountered in these boreholes penetrated through the terrace deposits. However, the depth of ground water based on the measurements in the water wells at the vicinity ranged between 55 and 60 m. Only in the boreholes drilled at the Bingöl High School site, groundwater depth was measured at a depth of 12 m below the ground surface. This water table is considered as a local water table. On the other hand, the groundwater in the boreholes drilled on the Bingöl Plain was encountered at a depth ranging between 1 and 14 m.



Figure 4.1: Göynük Brook (view from south-west towards north-east)



Figure 4.2: Gayıt Brook (view from SE towards NW)



Figure 4.3: Çapakçur Brook (view from west to east)

## 5 TECTONICS

Ketin (1973) initiated the first studies on the tectonic evolution of Turkey with his finding on the westward movement of the North Anatolian Fault (NAF) following the great Erzincan earthquake in 1939. His studies were later followed up and expanded by the next generation of Turkish earth scientists (Barka and Kadinsky-Cade 1988; Şengör 1979; Şengör and Yılmaz 1983; Aydan, 1997). The plate tectonics model of Turkey and its vicinity is shown in Figure 5.1. The tectonic evolution of Turkey was associated with the uplift of the Levantine Ocean base between Euro-Asia and Africa as a result of the northward motion of the Africa continent and Arabian plate (Ketin, 1973; Barka, 1997; Aydan, 1997). This phenomenon explains why the tectonic structure of the Anatolian plate consists of Anadolu mélange (Anatolides) and overlaying limestone-based sedimentary formations of Toros Mountains (Taurides) and Kuzey Anadolu Mountains (Pontides).

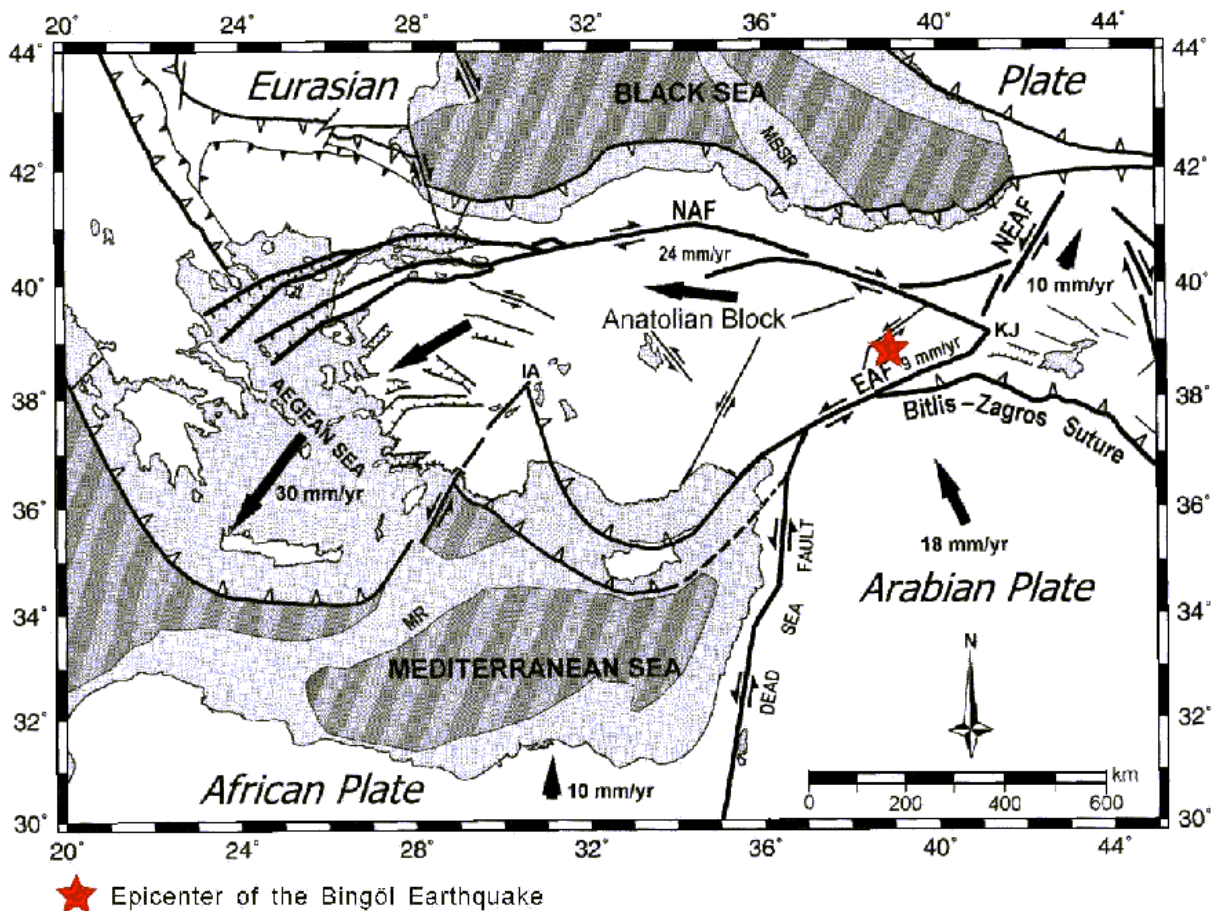


Figure 5.1: Main tectonic features of Turkey and its close vicinity (after Gülen et al. 2002)

The northward motion of the Arabian plate relative to Africa plate causes westward lateral movement (Barka, 1997) and anti-clock-wise rotation (Aydan, 1997) of the Anatolian block and the North-East Anatolian block to the east. The NAF zone and East Anatolian Fault (EAF) zone constitute the northern and southeast boundaries, respectively, of the westward moving and anti-clock-wise rotating Anatolian block. The motion of the Northeast Anatolian block is more complicated by extensive internal deformation of the block along conjugate faults. The NAF with a length of 1600 km runs through the Anatolia approximately in E-W direction and the EAF is a 550 km long, approximately northeast trending fault zone extending from Kargapazarı triple junction in the northeast to the Maraş triple junction in the southwest where it intersects the Dead Sea Fault. The earthquake-affected region is located at a tectonically very active part of Turkey and two main strike-slip faults, NAF and EAF are intersected (Figure 5.2). While NAF is a right-lateral strike slip fault zone, EAF is a left-lateral strike slip fault zone.

The EAF is composed of number of segments trending in NE-SW. Of the three segments are located earthquake region and its close vicinity. The northeastern segment of the EAF, called Göynük fault (Figure 5.2), consists of closely spaced parallel strike-slip faults appearing within a 2-3 km wide zone (Seymen and Aydın, 1972). This fault initiates at the south of Bingöl, shows morphological evidences in the vicinity of Sarıçiçek village, follows the valley of Göynük Brook (Figure 5.3a) and reaches to Kargapazarı at the northeast. It has a length of about 85 km. Arpat and Şaroğlu (1972) reported that left-lateral strike-slip of, at least, 15km is evident between Kargapazarı and Bingöl due to variations in drainage systems caused by the fault movements. A sub-parallel fault to the EAF is the Genç fault 20km south-east of Bingöl and is represented by the Genç fault, which is nearly parallel to the valley of Murat River as seen in Figures 5.2 and 5.3b.

The other segment of the EAF is called Palu fault extending to Hazar Lake. This segment probably extends beneath Bingöl and passes through Çevrîmpınar village. The sinistral slip of the fault was inferred by Arpat and Şaroğlu (1972) near Palu town about 22 km (Figure 5.3c). The strike of the fault in Palu town measured by the JSCE team is N67E and striations on the fault plane are  $7^{\circ}$  indicating a left-lateral slip with a slight vertical component.

There are also conjugate faults striking NE-SW and NW-SE parallel to the NAF and EAF, respectively, as shown in Figure 5.2. These faults bound the earthquake region from its south west and northwest. NE-SW trending faults, which possess left-lateral strike slip characteristics, are Sancak-Uzunpınar-fault, Kilisedere fault and Çevrîmpınar fault (Figure 5.2). Sancak-Uzunpınar fault, 40km long, shows a trend of N50E. This fault initiates near Sütgölü village at the south. The strike measured in this study at this village is N30E. As reported by Emre et al (2003), the southern part of the fault cuts volcanics and volcano-sedimentary rocks, and morphological features indicate evidences of its activity in Holocene and fault scarps (Figure 5.4a). Kilisedere fault is observed at the east of Sancak settlement (Figure 5.4b). The Çevrîmpınar fault striking N40E is about 20 km long and shows morphological evidents.

According to active fault map of Turkey (Şarođlu et al., 1992) Bingöl-Karakoçan fault and Sudüğünü fault are the right-lateral strike slip faults in the earthquake region (Figure 5.2). Bingöl-Karakoçan fault consists of two segments. The segment in the west strikes N70W, while the other passing near Bingöl trends in N50W. Sudüğünü fault zone has a length of 20km and its general trend measured by the authors near Sütgölü village is N70W (Figure 5.4c). Emre et al. (2003) reported that it is a 5 km wide fault zone. It terminates at the southern tip of Sancak-Uzunpınar fault in the vicinity of Sütgölü village.

The authors measured some fault outcrops during the investigation. The faulting mechanisms in the earthquake affected area were inferred from the measured fault striation data together with existing data by using the method proposed by Aydan et al. (2002) and plotted in Figure 5.5. As seen from the figure, the faulting mechanism are dominated by lateral-strike slip component. The lateral component are either sinistral or dextral. However, some thrust type faults are observed in the south of the region, which is closely affected by the Bitlis-Zagros Suture Zone (BZSZ).

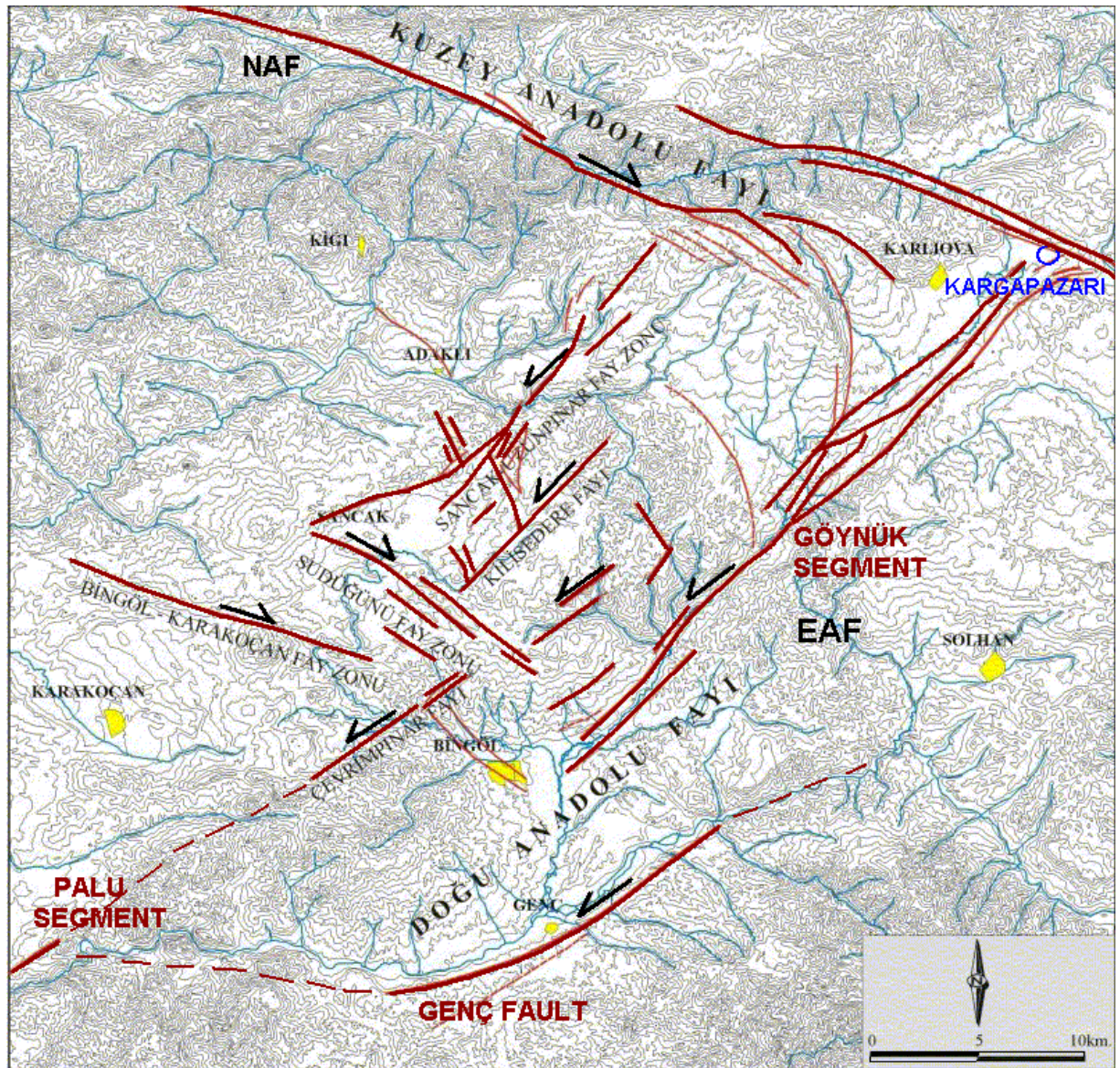


Figure 5.2: Active faults in earthquake affected region (modified from Emre et al. 2003)



(a) Göynük segment of the East Anatolian fault



(b) Genç fault



(c) Palu segment of the East Anatolian Fault

Figure 5.3: Some views of the faults in the earthquake affected region



(a) Sancak-Uzunpınar fault



(b) Kilisedere fault



(c) Sudüğünü fault (this fault assumed to cause the earthquake)

Figure 5.4: Some views of faults in the epicentral area

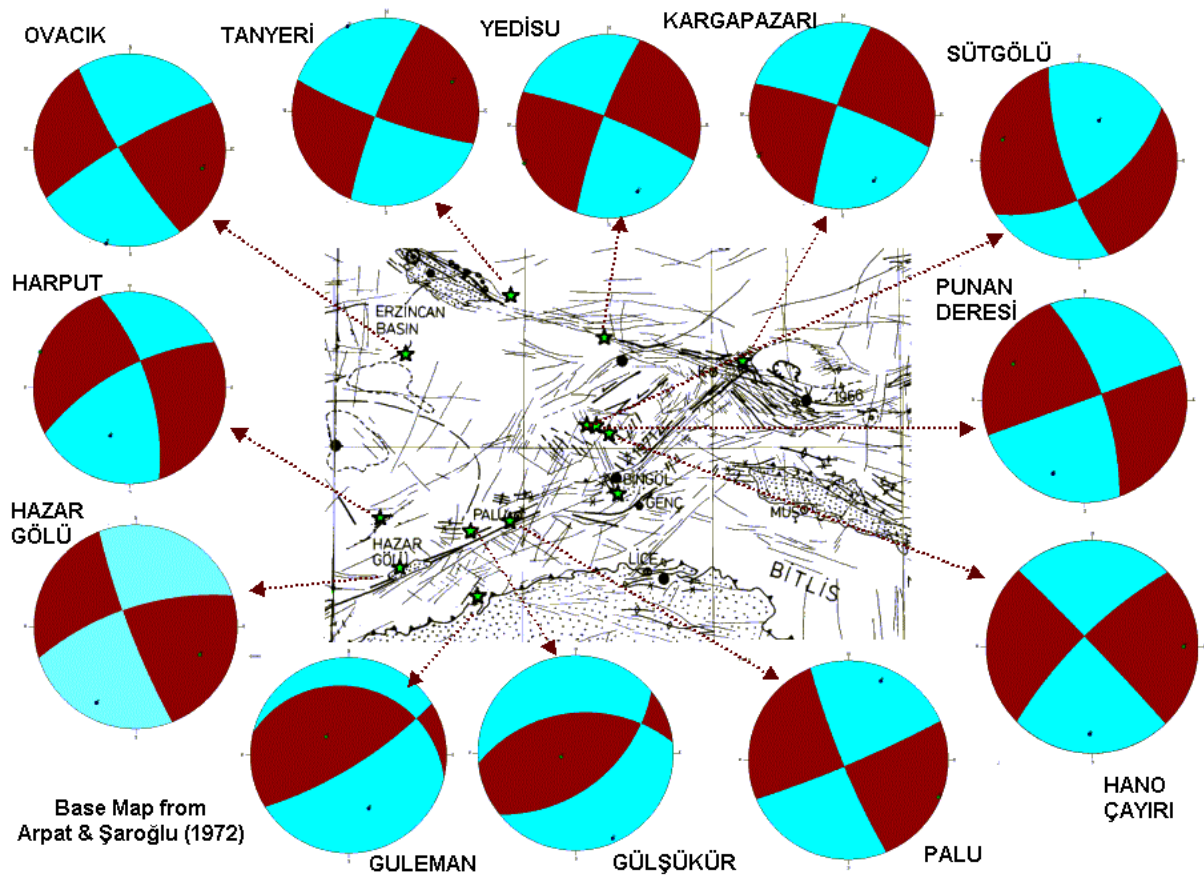


Figure 5.5: Faulting mechanisms inferred from the striation of the faults in the earthquake-affected region

## 6 SEISMICITY

Turkey is one of the seismically active countries in the world and situated on the Alpine Belt. The seismicity of Turkey is well documented for a period of 2000 years (Ergin et al., 1967). The distribution of the earthquakes with magnitudes greater than 4 for the period between 1900 and 2003 is shown in Figure 6.1. It is evident from this figure that the epicenters are concentrated along the NAF, EAF and West Anatolian Fault System (WAFS) and North-East Anatolian Fault (NEAF). The depth of hypocenters along the NAF and WAFS are generally between 10 and 30 km.

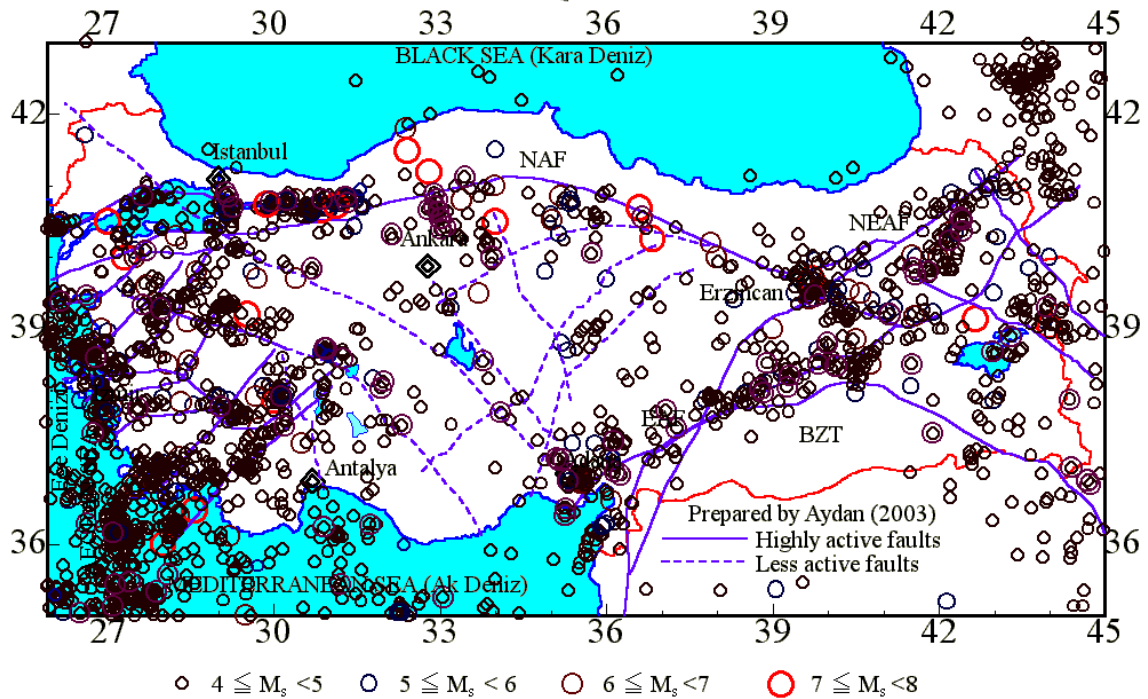


Figure 6.1: Seismicity of Turkey between 1900 and April 2003

Bingöl and its vicinity were assigned to the first-degree zone on the seismic risk map of Turkey prepared by the Earthquake Research Department of Turkey. Active faults surrounding the Bingöl region indicates that the region is a highly earthquake-prone area. In the last century, many earthquakes affected particularly the vicinity of Erzincan, Bingöl and Tunceli. These earthquakes with magnitudes greater than 5 are shown in Figure 6.2. The 1957 ( $M_s=5.1$ ), 1968 ( $M_s=5.7$ ) and 1995 ( $M_s=5.7$ ) Kiğı earthquakes and May 22, 1971 ( $M_s=6.8$ ) Bingöl earthquake are the earthquakes resulted in loss of life and heavy damages in the

studied earthquake region. However, among those, the Bingöl earthquake occurred on May 22, 1971 at 6:45 pm on local time was the most destructive earthquake. Figure 6.3 shows the locations and focal mechanisms of earthquakes since 1939 in the earthquake affected region. The earthquakes along the NAF and EAF are caused by lateral strike-slip faulting. On the other hand, the earthquakes along Bitlis-Zagros Suture and away from the NAF exhibit thrust type faulting with a sinistral or dextral sense of lateral deformation. The focal mechanisms shown in Figure 6.3 resemble to those inferred from fault striations as shown in Figure 5.5.

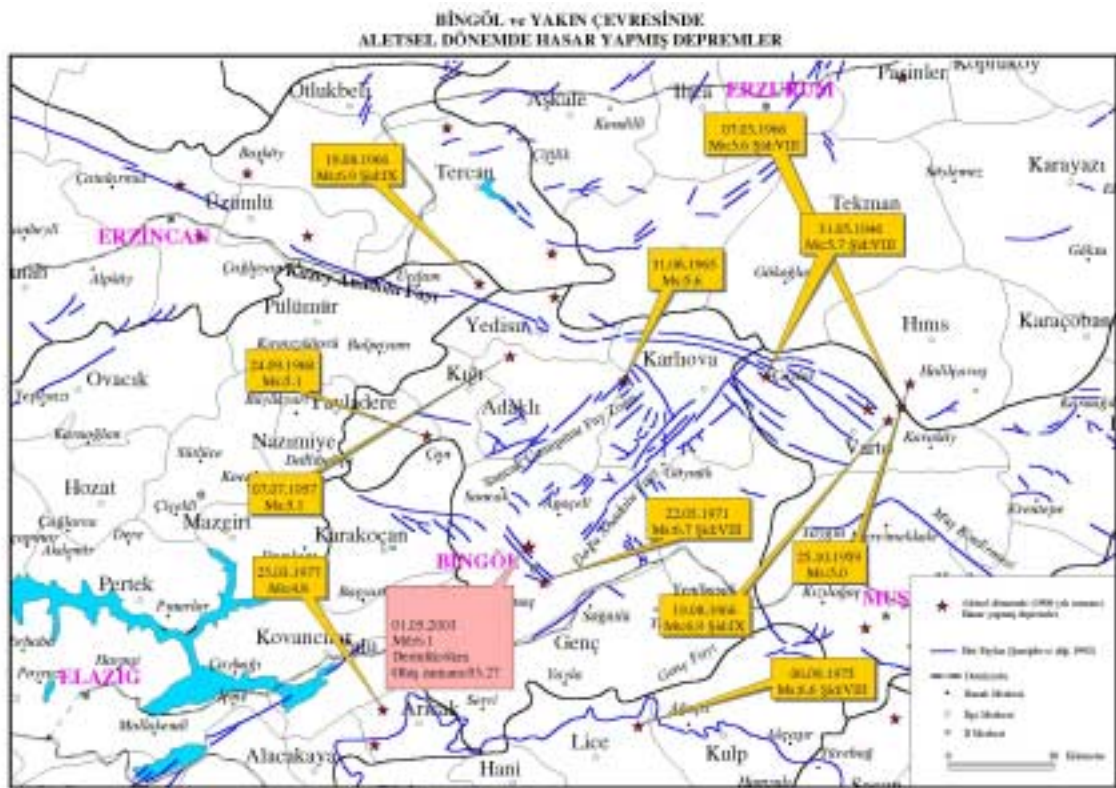


Figure 6.2: Locations and magnitudes of earthquakes in the region (DAD-ERD, 2003)

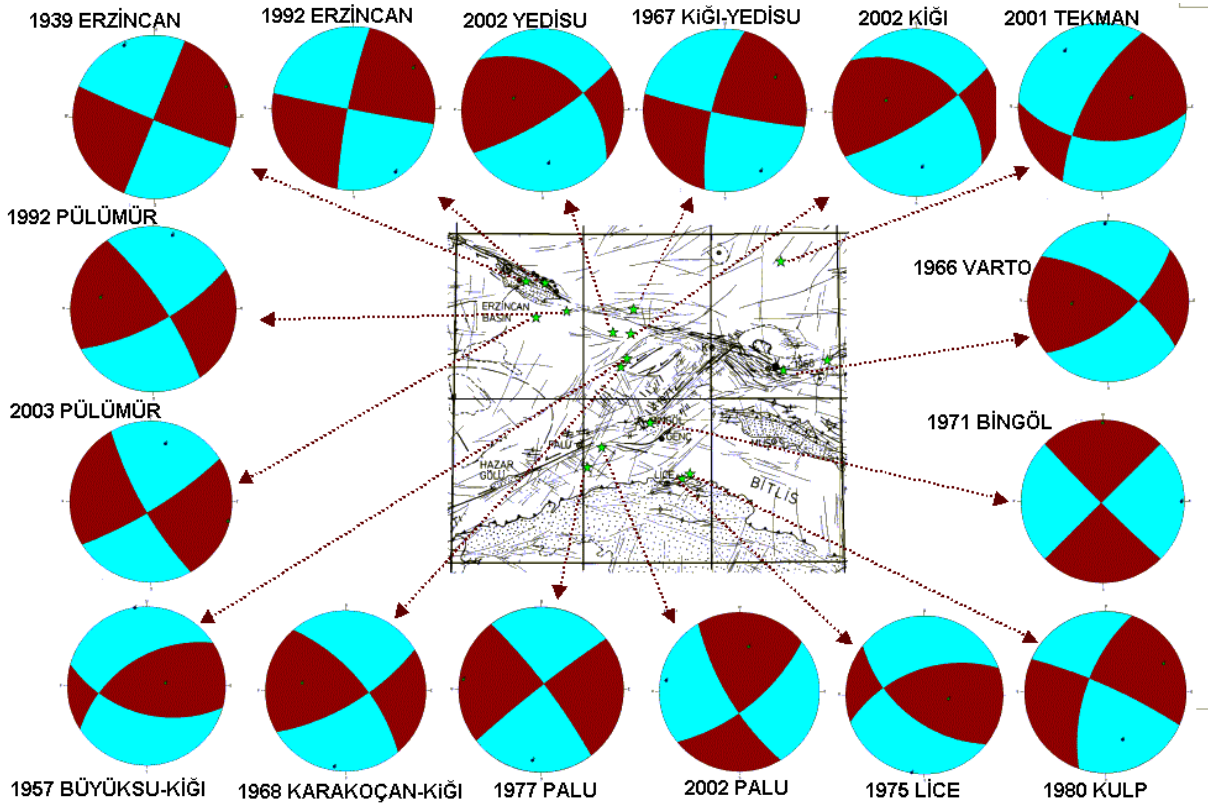


Figure 6.3: Focal mechanisms of the earthquakes in the earthquake affected region

The 1971 earthquake with a magnitude ( $M_s$ ) of 6.8 caused a total loss of 755 people and heavy damages particularly in Bingöl city. About 5323 buildings collapsed and heavily damaged (Aktan et al., 1972). Based on the instrumental data of USGS (Aktan et al., 1972), its epicenter was located at 10 km south of Bingöl, and depth of its focus was 3 km, While macroseismic observations indicated that the epicenter was 10-12 km at the east of Bingöl (Aktan et al., 1972; Seymen and Aydın, 1972). Aktan et al. (1972) reported that a strong foreshock, which was felt in the close vicinity and caused some damages, occurred on May 22, 1971 at 11:26 am on local time. The causative fault of this earthquake was the Göynük segment of the EAF and its southern part of this fault with a length of 35 km was broken during the earthquake (Seymen and Aydın, 1972). Based on the Mercalli scale, the intensity of the earthquake was estimated as VIII by Seymen and Aydın (1972), and a zone between Bingöl at southwest and Ilıca located near Göynük Brook at northeast subjected to heaviest damage. En-echelon surface ruptures and slip zones particularly at the epicentral area between Çeltiksuyu and Ilıca were observed. Their trend was between N25-45E and length varied

between 50 and 500 m as reported by Seymen and Aydın (1972) and Arpat and Şaroğlu (1972). These investigators also noted that although small vertical drops along the slip zones appearing on inclined topography were observed, the absence of vertical drops along the surface ruptures occurred on flat areas indicated that the causative fault had almost a horizontal component (Figure 6.4a). In addition, sand ejections along some surface cracks were observed at some locations in the alluvial sequence such as near Göynük Brook and Çeltiksuyu Brook as seen in Figure 6.4b (Aktan et al., 1972). Similarly to those observed in the recent Bingöl earthquake of 2003, landslides and rock falls were also observed on the slopes of Göynük Brook, Kös stream, and Bilaloğlu and Elmalı villages (Figure 6.4c,d).

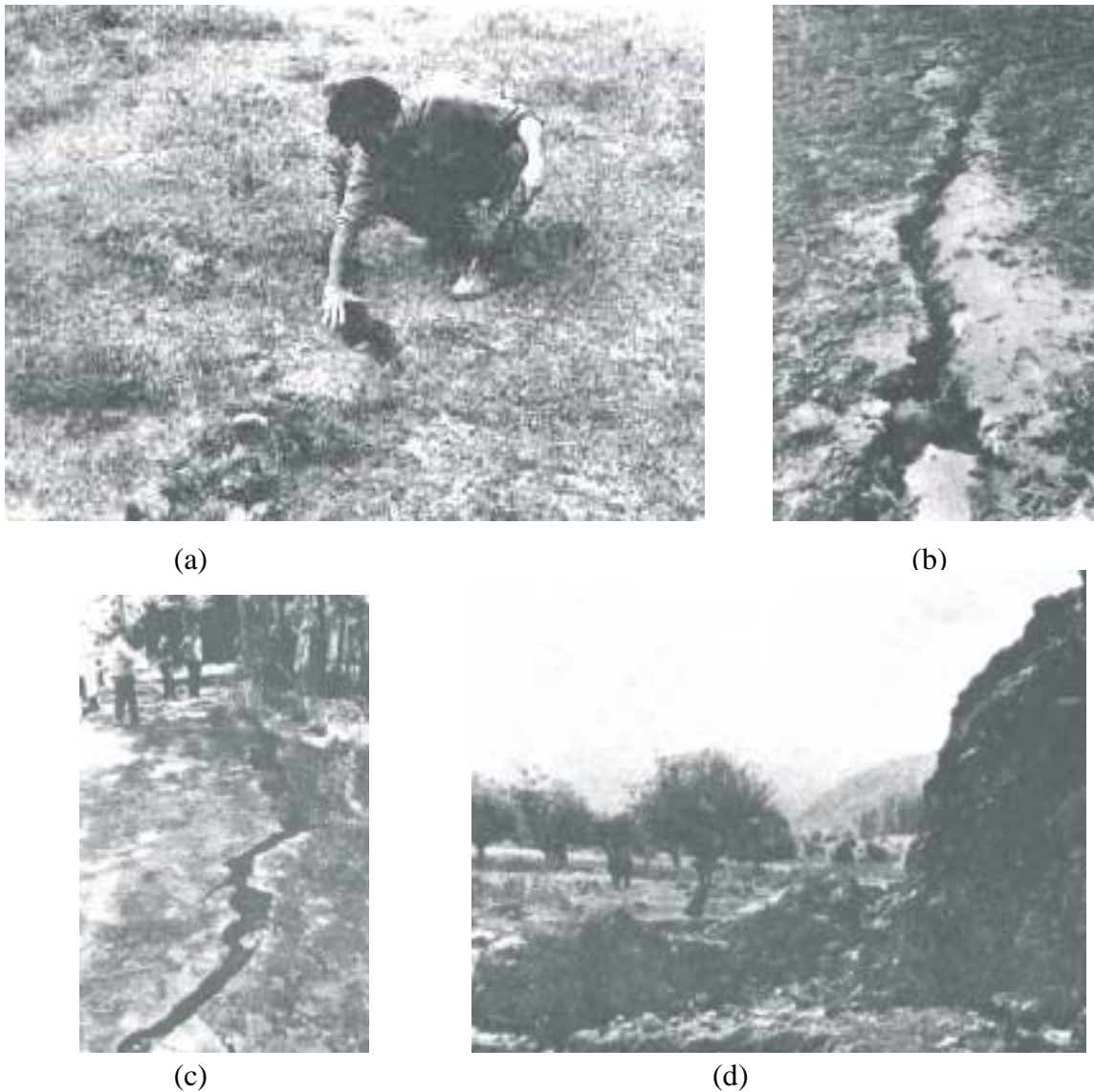


Figure 6.4 Some views of surface fractures and liquefaction and slope failures caused by the 1971 Bingöl earthquake (after Aktan et al., 1972)

## 7 CHARACTERISTICS OF THE EARTHQUAKE, STRONG GROUND MOTION AND FAULTING

### 7.1 Main Characteristics of the Earthquake

The main shock of the Bingöl earthquake occurred at 03:27 on Turkish Standard Time (TST) on May 1, 2003. Various institutes in Turkey and other countries determined the hypocenter of the earthquake and its faulting mechanism. The locations of the epicenters predicted by various institutions, which are mostly scattered at the north of Bingöl City, are shown in Figure 7.1. Table 7.1 compares the hypocenter parameters of focal plane solutions. The focal plane solutions (Figure 7.2) suggest a right-lateral strike slip fault. However, they indicate two possible faults striking in NW-SE and NE-SW. The focal depths computed by several Institutes range between 5 and 15 km.



Figure 7.1 Comparison of estimated epicenters of the earthquake by various institutes

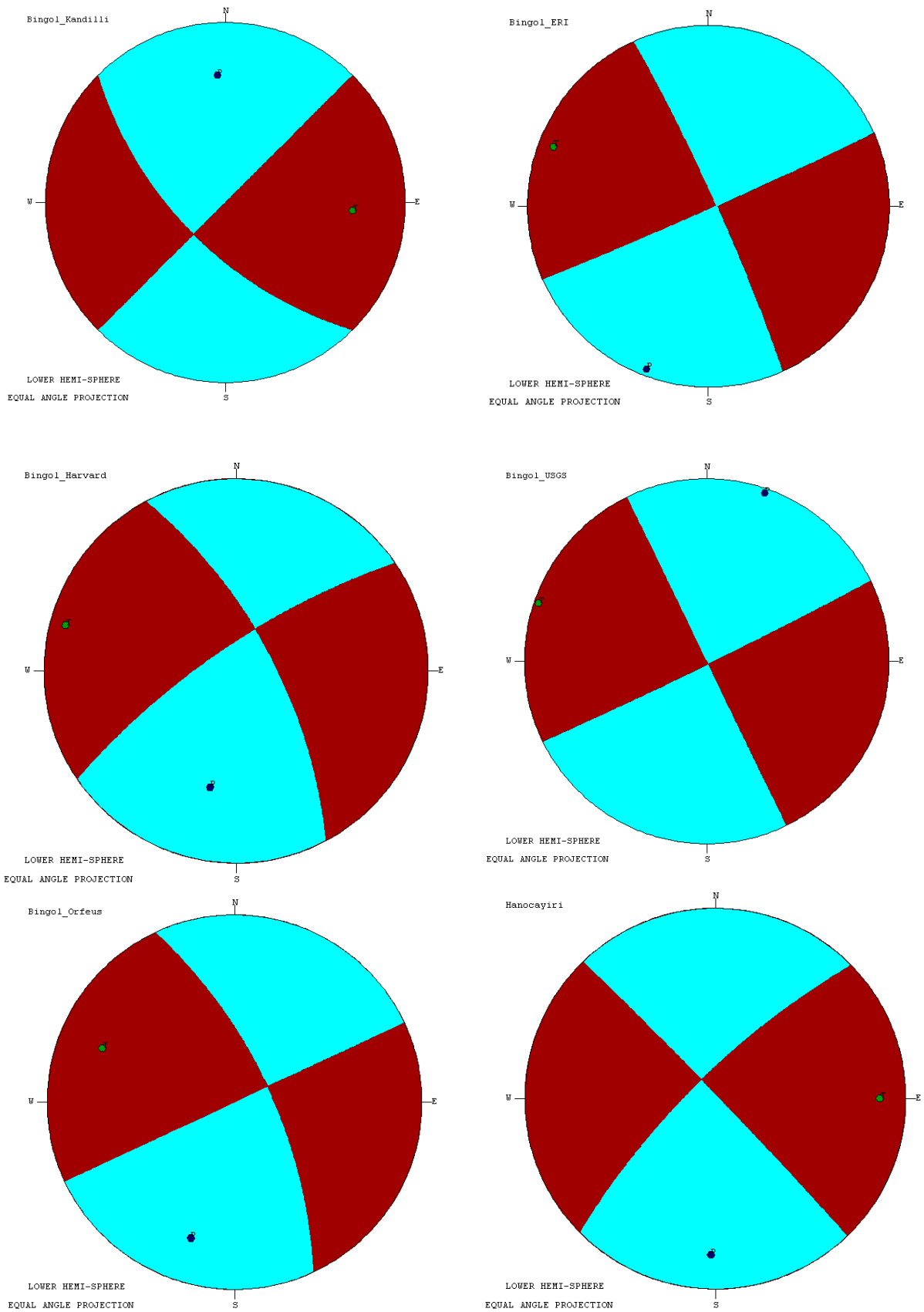


Figure 7.2: Focal plane solutions by various institutes together with a faulting mechanism inferred from the ground surface rupture at Hano-Çayırı

Table 7.1: Parameters of the earthquake estimated by different institutes

Institute	Latitude	Longitude	Depth(km)	Magnitude	Strike	Dip	Slip
KOERI	39.01	40.49	10	Ms=6.4	NP1 225° NP2 135°	90° 62°	28° 180°
DAD	38.94	40.51	6	Md=6.1			
USGS	38.99	40.46	10	Mw=6.4	NP1 64° NP2 154°	88° 90°	0° -178°
HARVARD	39.01	40.53	15	Mw=6.3	NP1 332° NP2 236°	68° 75°	-164° -22°
ORFEUS	38.74	40.60	24	Mw=6.6	NP1 335° NP2 65°	68° 90°	180° 22°

## 7.2 Aftershocks

Before the 2003 Bingöl earthquake, the seismic network was not dense. After the earthquake, several temporary seismic stations have been installed for observation of aftershocks in Bingöl and six small settlements in its vicinity by the ERD (2003), Turkish Scientific Research Council-Marmara Research Center (TÜBİTAK-MAM, 2003), KOERI and Istanbul University, respectively. More than 6000 aftershocks occurred. The records released by KOERI (2003) 19 days after the earthquake suggest about 400 aftershocks with  $M > 4$  between 40.20 and 40.65 longitudes and 38.80 and 39.25 latitudes. Figure 7.3 shows the aftershocks during the first 3 days. As seen from the figure the aftershocks took place over a large area around the epicenter of the main shock between the NE-SW and NW-SE striking faults. This situation makes it difficult to estimate an evident faulting trend. However, the distribution of the aftershocks with magnitudes greater than 4.0 shows a trend in NW-SE direction, which has a good agreement with one of two faults striking in NW-SE as obtained from focal plane solutions (Figure 7.2).

As expected, the number of aftershocks tends to become stationary as time goes by. Figure 7.4 shows the number of shocks per day and cumulative number of shocks as a number of the elapsed day after the main shock for about 7 days.

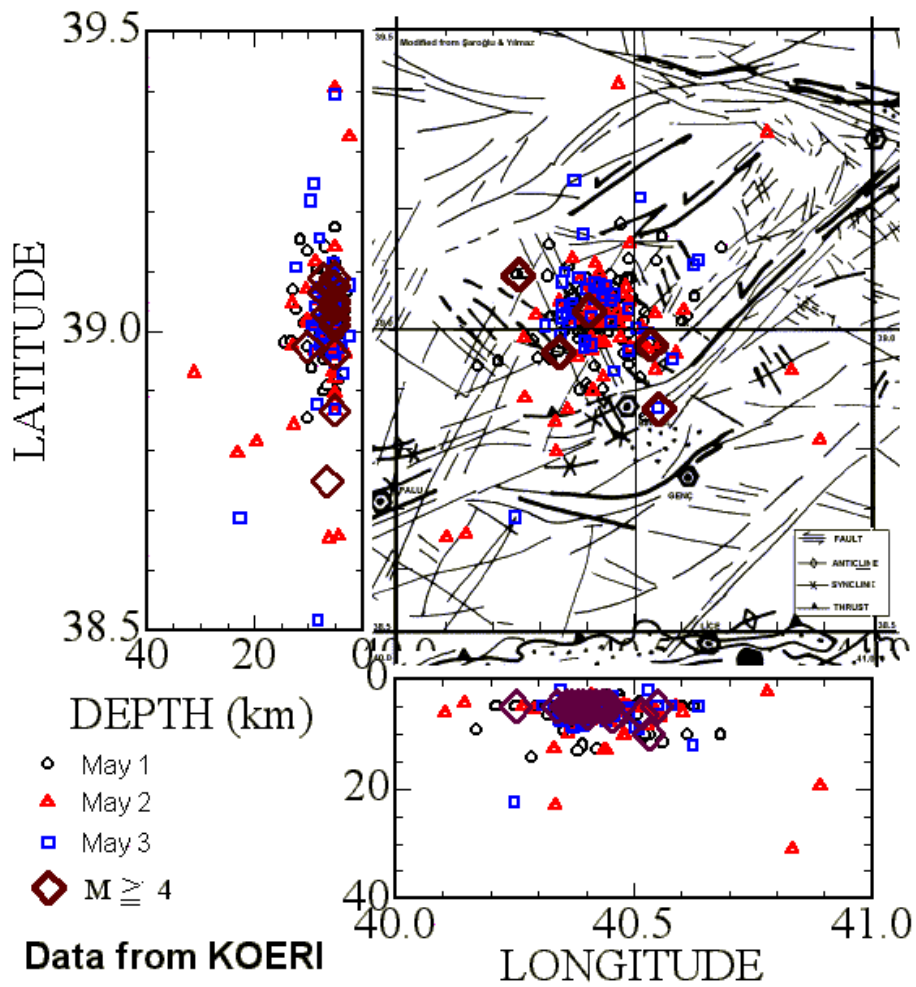


Figure 7.3: Locations of aftershocks

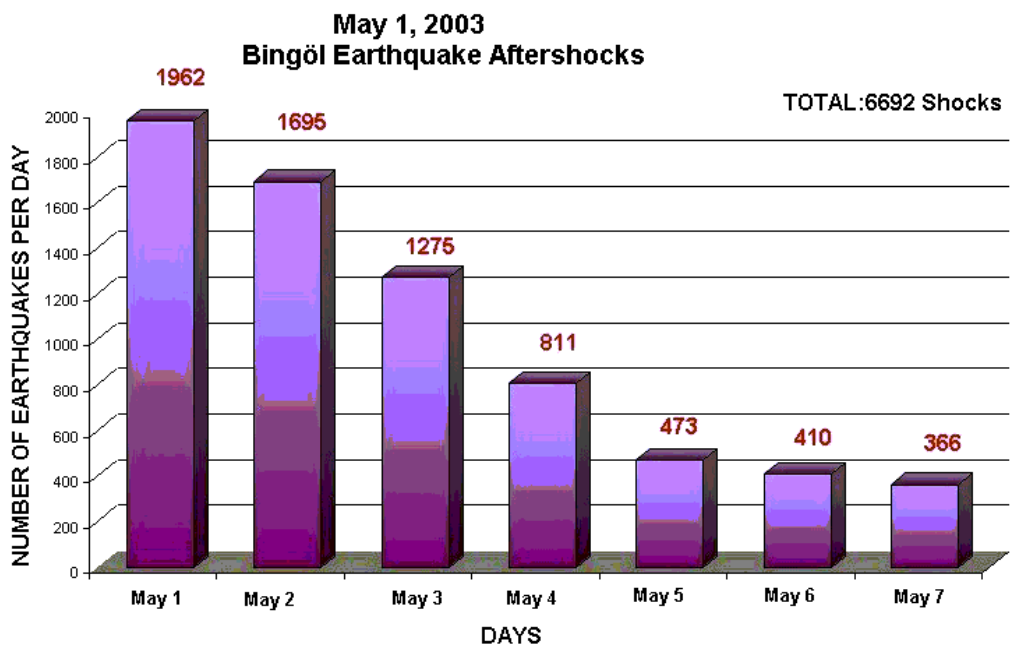


Figure 7.4: Variation of aftershocks as a function of time (modified after KOERI, 2003)

### 7.3 Strong Ground Motion of the Main Shock

The region has been instrumented with a strong motion network operated by the Earthquake Research Department (ERD). The strong motion network of the (ERD) has stations at Bingöl (BNG), Elazığ (ELZ), Tercan (TER), Erzincan (ERC) and Tatvan (TVN) in the close vicinity of the earthquake region. The strong motion records from this network can be easily accessed through INTERNET. The main shock of the earthquake was recorded by a GRS-16 type accelerometer in the building of Bayındırlık İskan Müdürlüğü at Bingöl (Figure 7.5a). This building is a one-story building, which is adjacent to the 4-story main building (Figure 7.5b). The accelerometer was mounted in a direction of N21E on a concrete base directly founded onto ground as shown in Figure 7.5c. Although there is no direct available information about the soil type beneath the accelerometer, this part of the city is founded on stiff terrace deposits. Figure 7.6 shows NS, EW and UD acceleration records at Bingöl station. The largest acceleration recorded at this station is 545.5 gal in NS direction. The UD component of the earthquake is also quite high probably due to one of the characteristics of inland earthquakes. The accelerations recorded at other stations in the region are given with those from BNG station in Table 7.1. It is not known that if the existence of adjacent 4-story building or topographic effects played some roles on the high acceleration at Bingöl station. Nevertheless, the model experiments by Aydan on rock slopes clearly showed that accelerations are larger at the top of the slope and they are amplified near the slope crest (Figure 7.7). Figure 7.8 shows the attenuation of maximum ground acceleration as a function of distance and S-P time difference. The plotted results suggest that the following relation between S-P time difference and hypocenter distance may exist for Turkish earthquakes:

$$R = k\Delta\tau$$

where  $\Delta\tau = t_s - t_p$  and  $k$  may be regarded as Omori coefficient. The value of parameter  $k$  may range between 8.7 and 9.6. Fourier spectra of each component at BNG station are shown in Figure 7.9. Figure 7.10 shows the traces of acceleration waves on the horizontal plane at BNG station, which is the closest station to the epicenter. It can be seen from Figure 7.10 that initially the highest shaking magnitudes are in SE10 direction. From this figure, one may also infer possible directions of toppling and shearing structures and slope and ground failures.

Table 7.1: Maximum accelerations of the Bingöl earthquake of May 1, 2003 measured at various stations in the earthquake region.

Station name	Acceleration (gal)			Distance to epicenter (km)	S-P Time Difference (s)
	N-S	E-W	UD		
BNG	545.53	276.82	472.26	14	1.55
ELZ	8.00	7.00	5.00	120	16.24
TER	5.10	10.30	4.30	86	12.28
ERC	8.34	7.50	4.11	112	16.36
TVN	5.98	4.24	2.90	176	22.66
MLZ	5.00	5.50	3.00	186	-

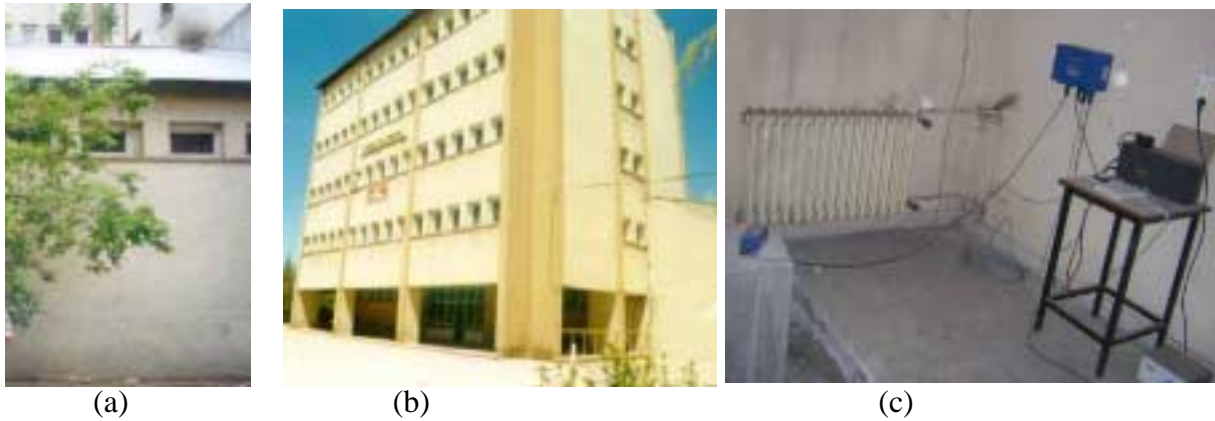


Figure 7.5: Views of the strong motion recording station and its environment

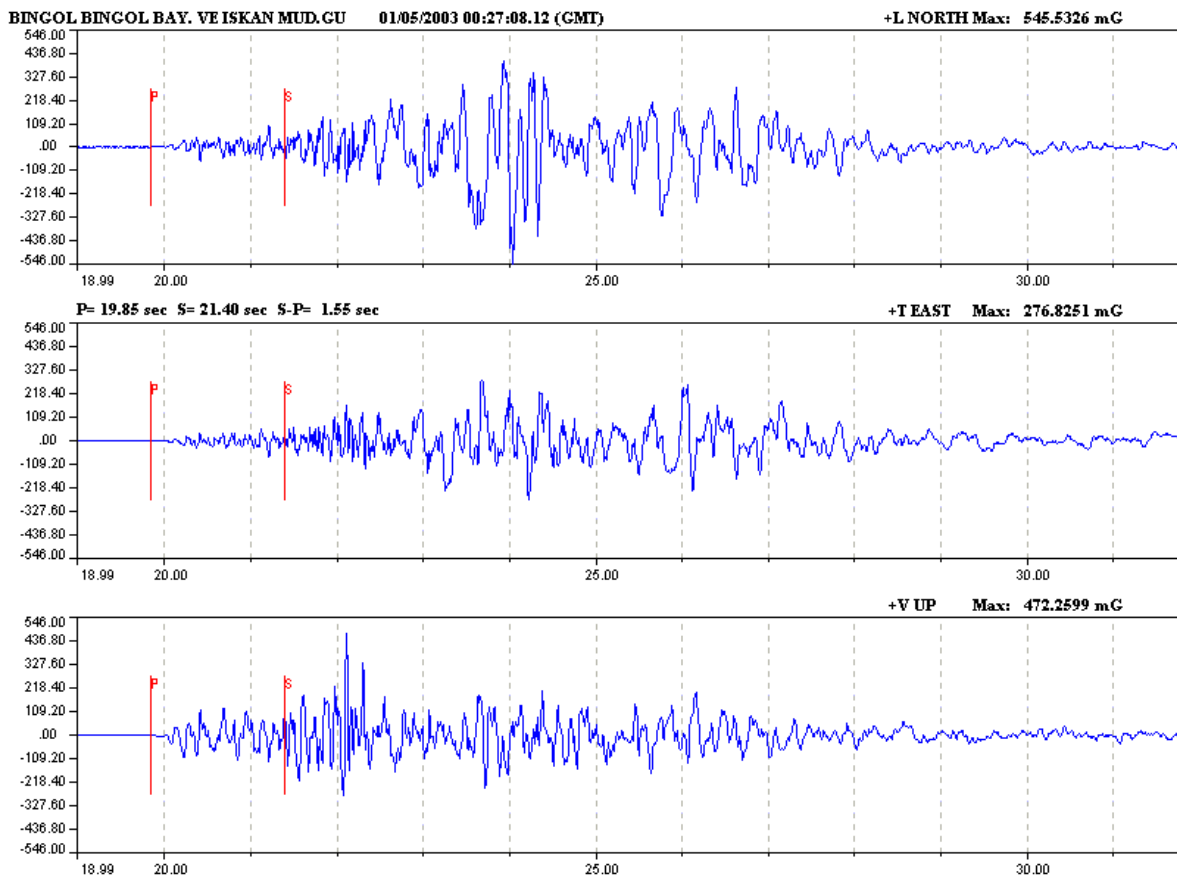


Figure 7.6: Acceleration records measured by DAD/ERD at Bingöl

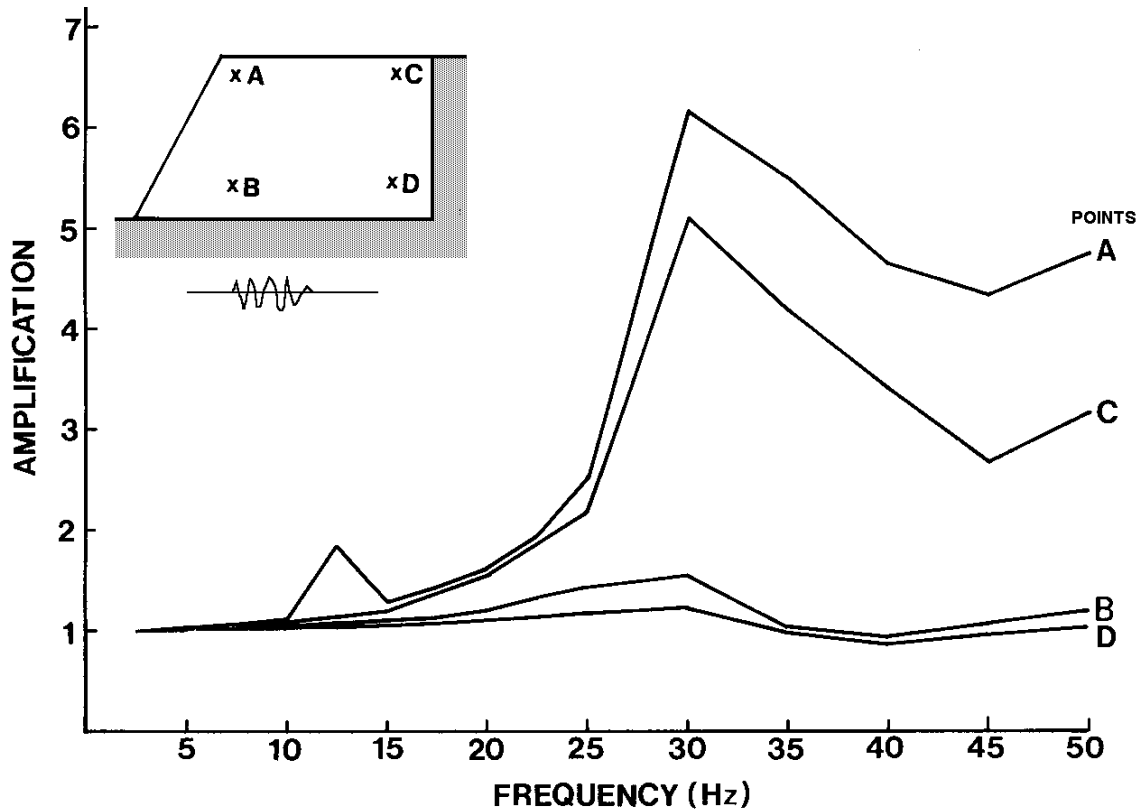


Figure 7.7: Variation of peak accelerations as a function of position within a model slope

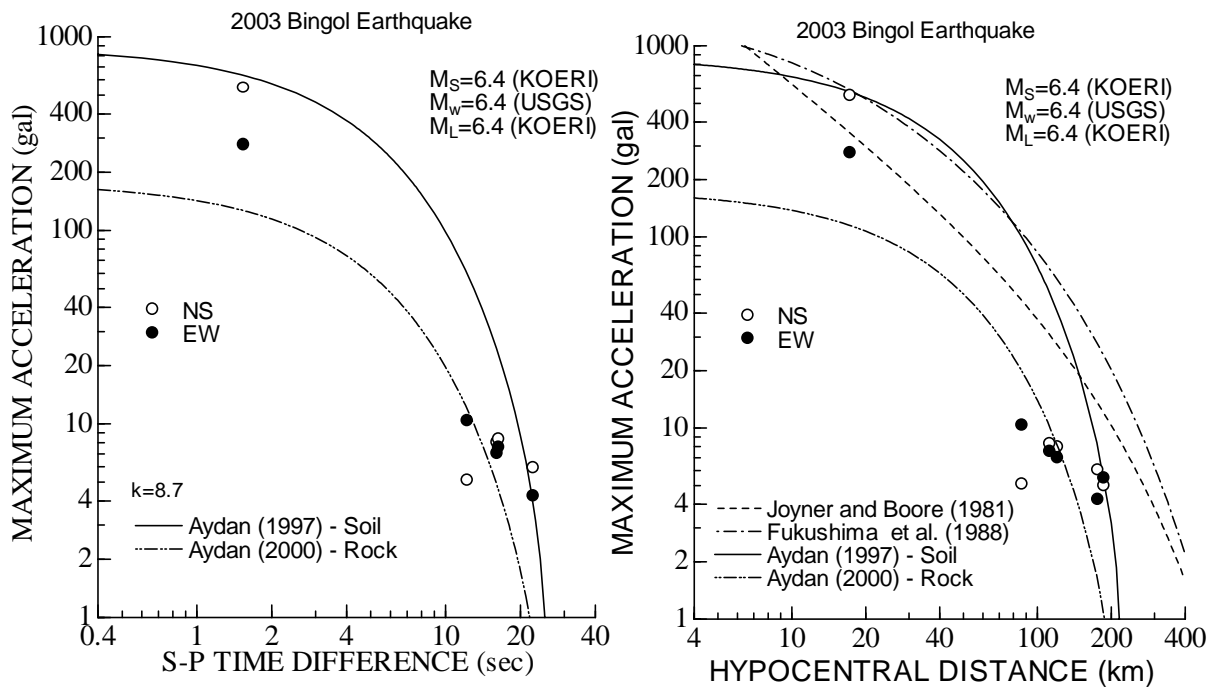


Figure 7.8: Attenuation of the maximum ground acceleration with distance

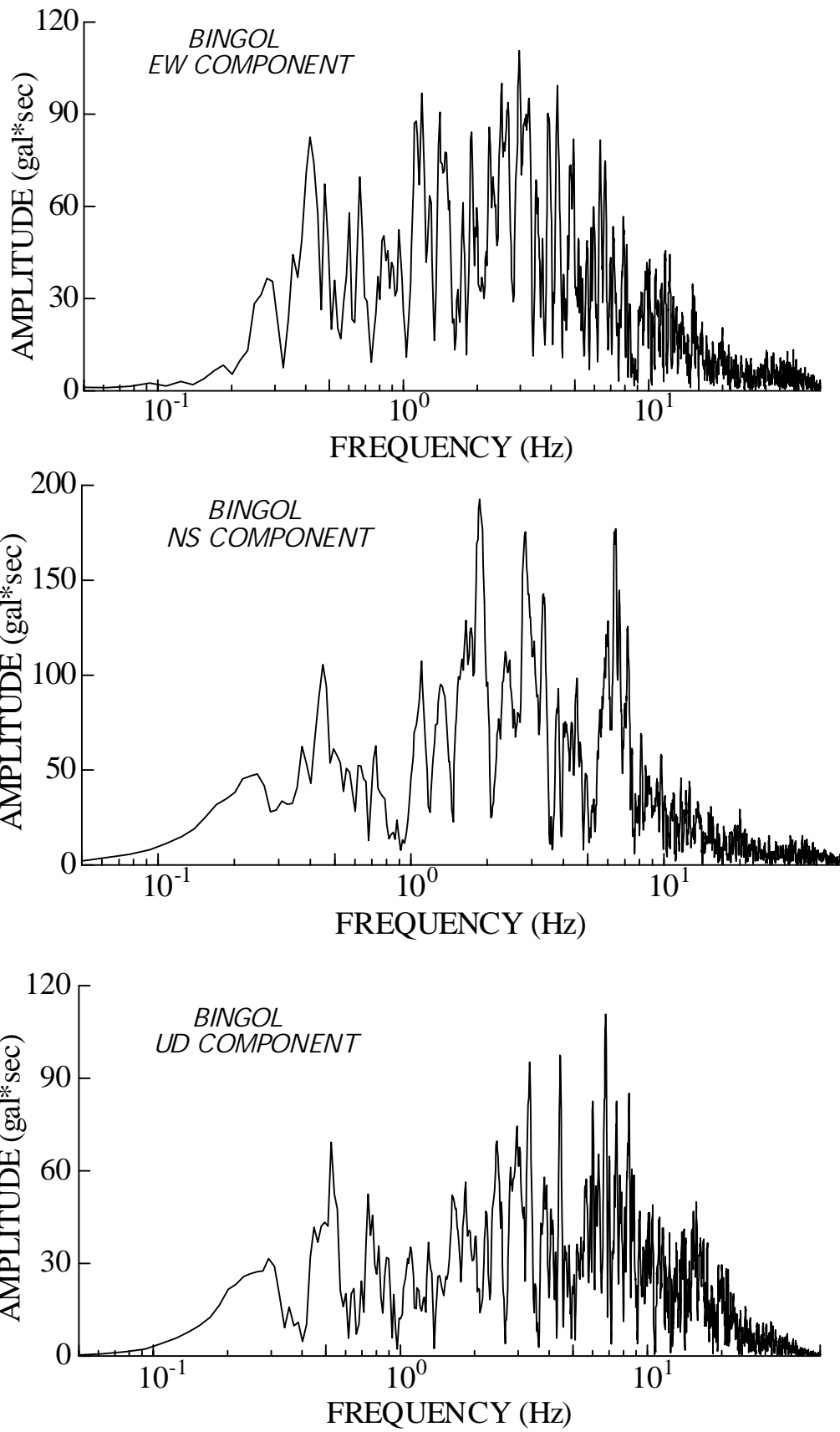


Figure 7.9: Fourier spectra of Acceleration records measured by DAD/ERD at Bingöl

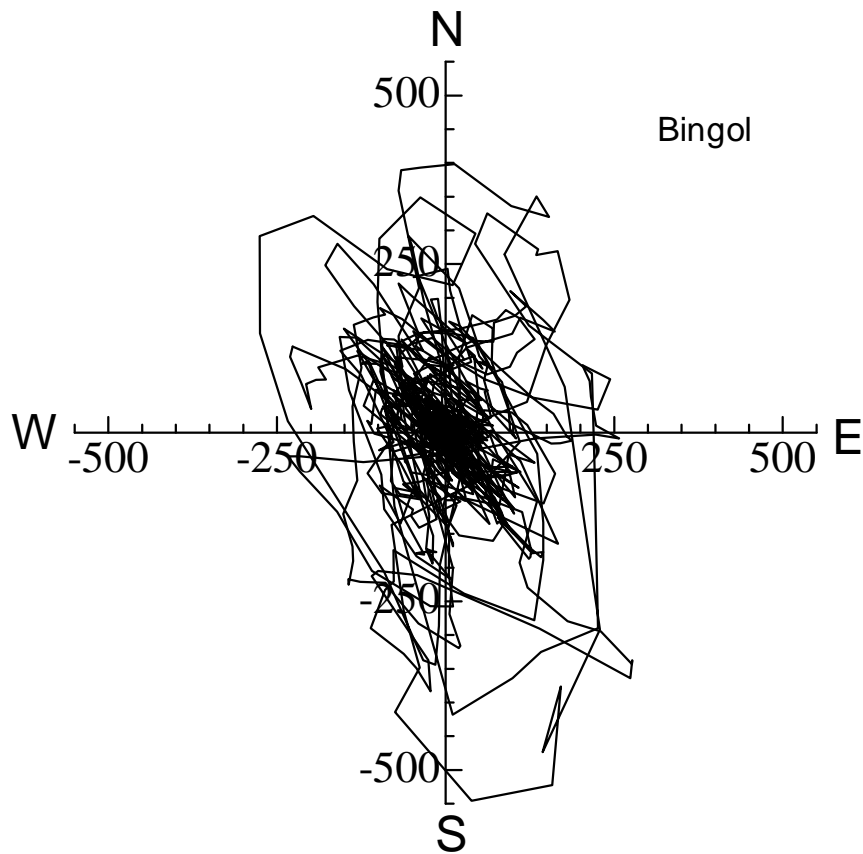


Figure 7.10: Trace of acceleration response on horizontal plane

#### 7.4 Response Spectra of Strong Motions

Although many stations of the National Strong Motion Network recorded the main shock, the records of Bingöl station are only selected since they represent the shaking situations in Bingöl City and nearby town and villages. The acceleration spectra of the main shock are shown in Figure 7.11 for the records taken at Bingöl. The value of damping coefficient was set to 0.025 and 0.05 in computations. The acceleration response spectra for EW component show peaks at periods varying between 0.075-0.86s. The dominant period seems to be between 0.15s and 0.32s, which was observed in the previous earthquakes in Turkey. As for NS acceleration spectra, the peak is observed at 0.15seconds. The peaks of the UD acceleration spectra appear at 0.055 and 0.12 seconds. Particularly, the largest peak occurs at 0.12s at Bingöl station, which implies that buildings having one or two stories could had been subjected to very severe vertical shaking. From acceleration response spectra and natural periods of structures in Turkey, it may be inferred that buildings having 2-3 stories in Bingöl should be subjected to severe shaking.

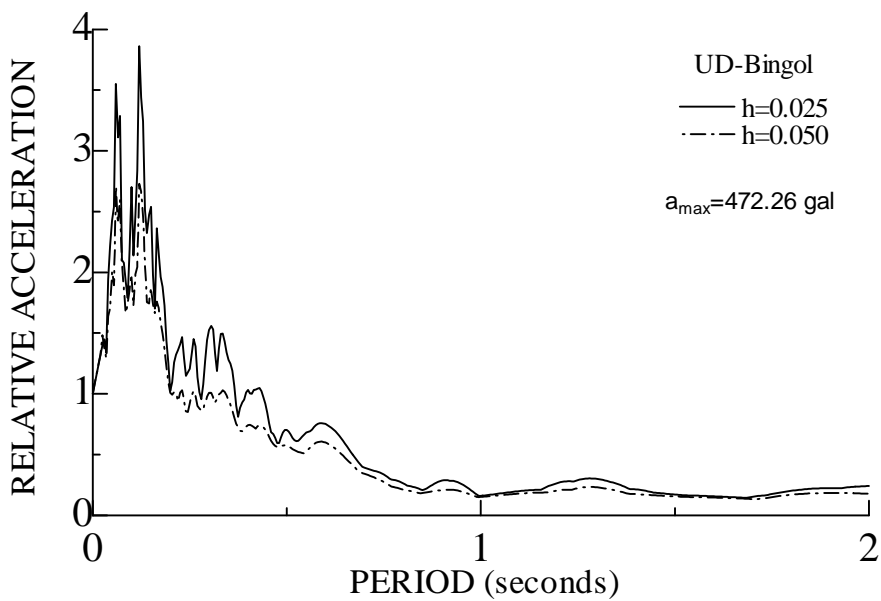
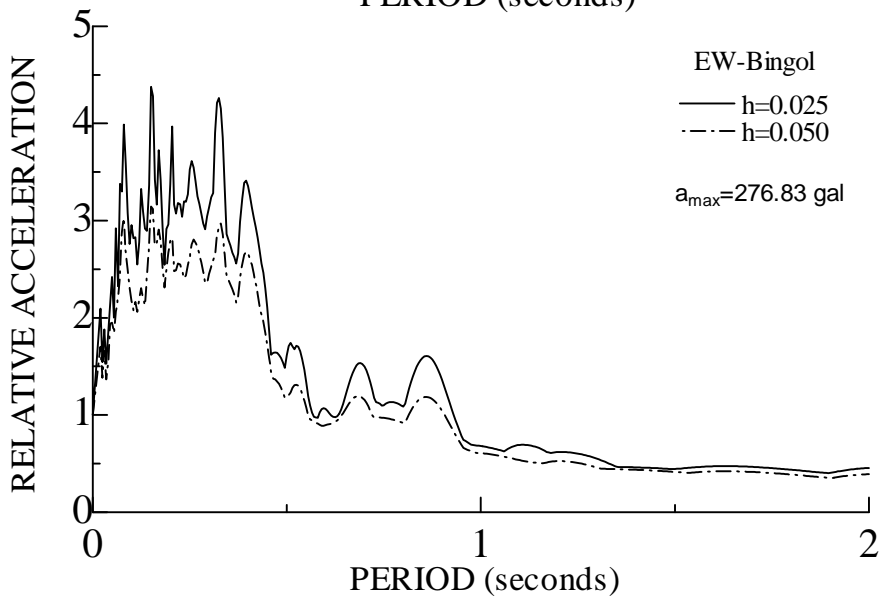
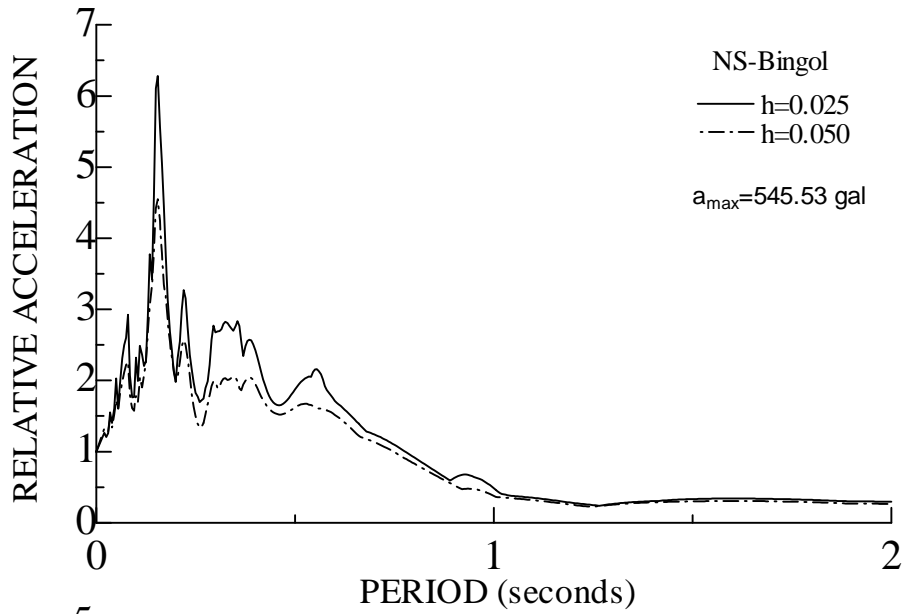


Figure 7.11: Acceleration response spectra of records at Bingöl

## **7.5 Surface Rupture Traces**

On the contrary to very long and evident surface rupture traces observed in the 1999 Kocaeli and Düzce (Aydan et al., 1999, 2000) and in the 2002 Çay-Eber earthquakes of Turkey (Ulusay et al., 2002), this recent earthquake did not cause any evident rupture trace. However, a few short cracks trending in N44-60W were observed at a location called Hanoçayırı between Sudüğünü and Oğuldere villages by the JSCE team (Figure 7.12a). About 20cm right lateral and 1-6 cm downward movements of the southern block of these cracks were observed (Figure 7.13). In a shallow and narrow trench, which was excavated by Ö. Emre from the General Directorate of Mineral Research and Exploration of Turkey (MTA), the crack observed at the surface seems to be continuous with depth (Figure 7.12b, c). A water well of 6 m deep located at 20 m west of this crack collapsed during the earthquake. Towards west, a similar crack appears and terminates in a short distance (Figure 7.12d). The separation crack in the walls of a house made of stone blocks 100 m away along the alignment of this surface crack was also observed (Figure 7.12e). The other group of surface cracks was observed at the southern margin of a flow triggered by the earthquake at the same location (Figure 7.13). Their trend was in N30E direction and vertical drops between 1 and 3 cm were observed. Total length of these cracks was 250 m. Two parallel cracks were evident from place to place. However, these cracks can not be directly associated with the Sudüğünü fault due to their general trend, topographical conditions and their very close position to the mass movement.

## **7.6 Directions of Collapse**

Collapse directions of buildings, minarets, garden walls and chimneys were measured by the JSCE team at some settlements, particularly in Bingöl, and are plotted in Figure 7.14. Distribution of collapse directions in Bingöl is generally concentrated in SE and NE directions. However, a few collapses are in SW and NW directions. At the north of Bingöl near to the epicenter (in Çimenli and Sudüğünü villages) different directions of collapses in SW, SE, NE, and NW were measured (Figure 7.14b). Some typical examples of collapses are shown in Figure 7.15.



(a)



(b)



(c)



(d)



(e)

Figure 7.12: Some views of surface cracks at Hanoçayırı



(a)



(b)

Figure 7.13: Some views of cracks at the site of lateral spread at Hanoçayırı

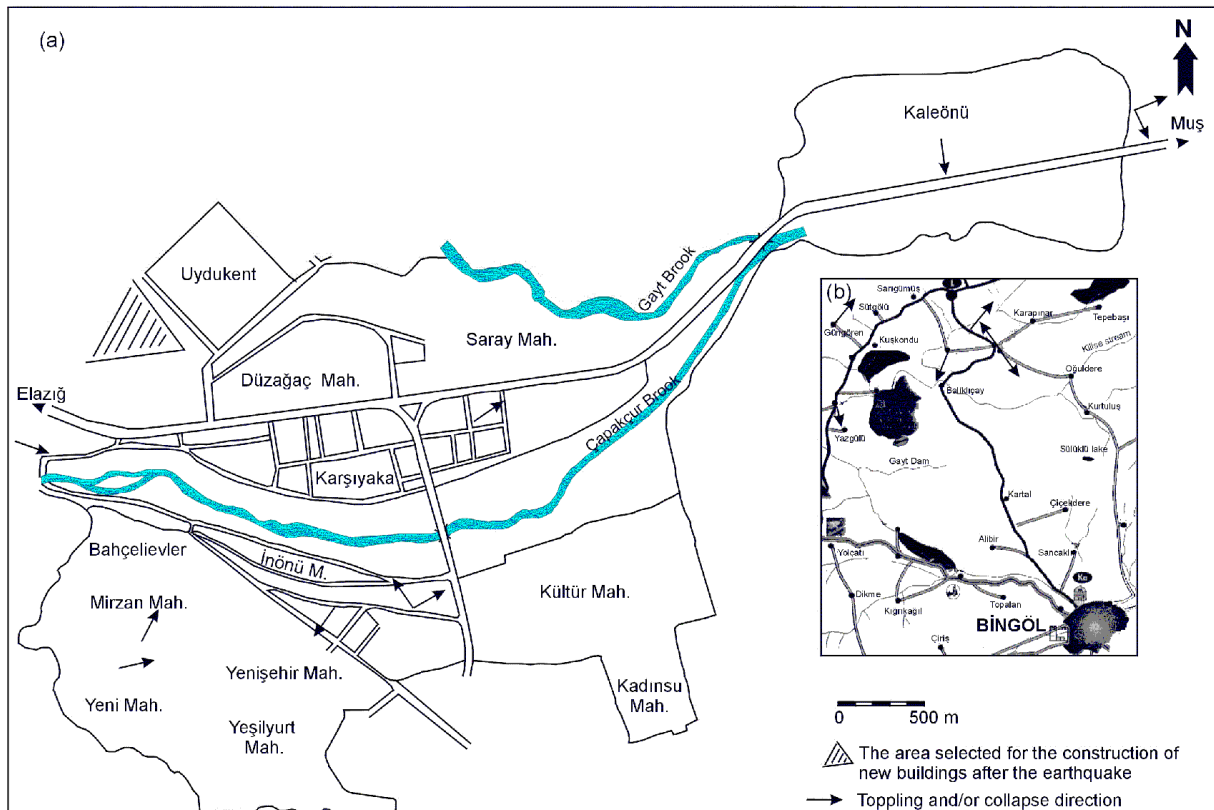


Figure 7.14: Directions of collapses or toppling in the earthquake affected region

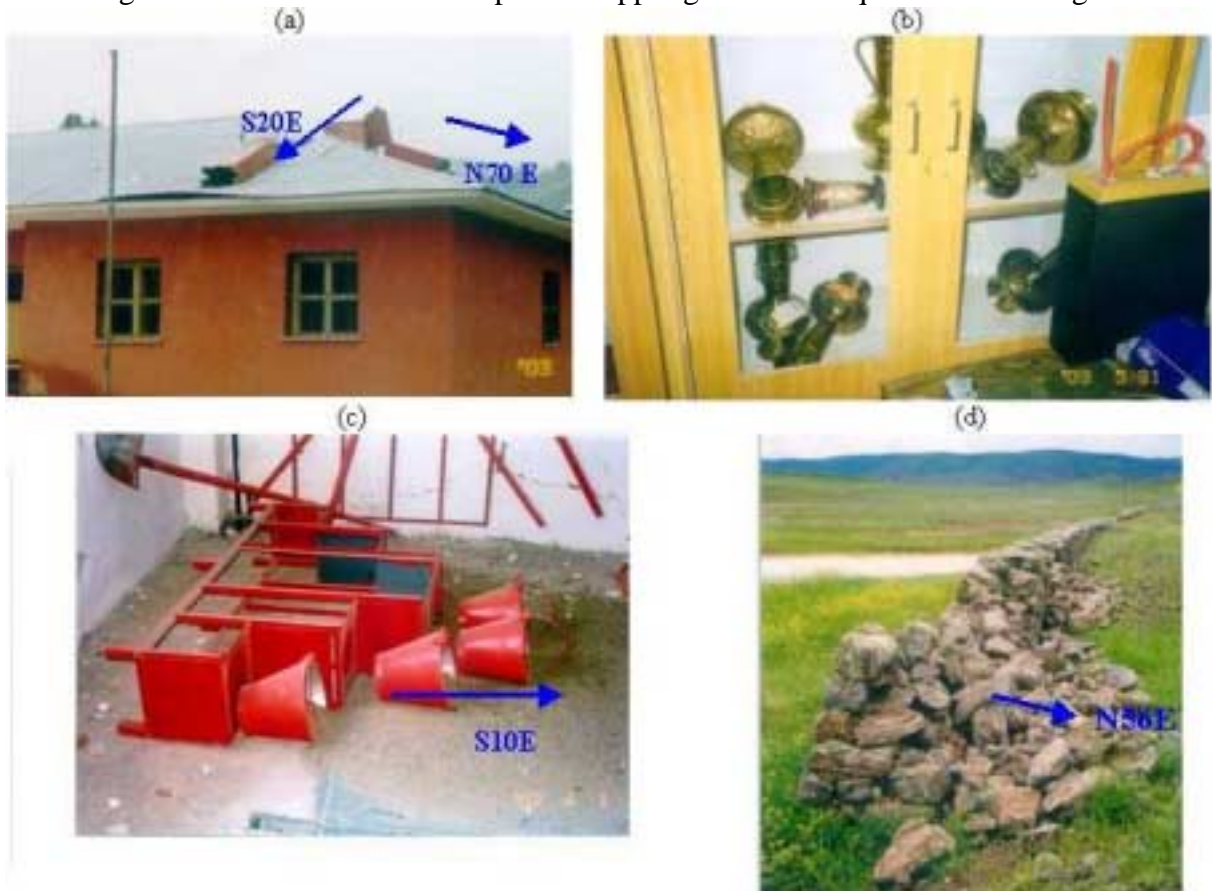


Figure 7.15: Some examples of collapses

## 8. GEOTECHNICAL ASPECTS OF THE EARTHQUAKE

In this chapter, the geotechnical aspects of the May 1, 2003 Bingöl earthquake by emphasizing local site effects and seismically induced ground deformations such as landslides, liquefaction and liquefaction-induced lateral spreading are presented and discussed. For this purpose, in addition to the observations both in Bingöl city center and in the epicentral area, available records of geotechnical boreholes 10-15 m deep drilled at Bingöl and its close vicinity for ground investigations, and observation trenches opened (Figure 8.1) near collapsed and heavily damaged buildings, and data from two shallow boreholes at Hanoçayırı lateral spreading site were also evaluated.

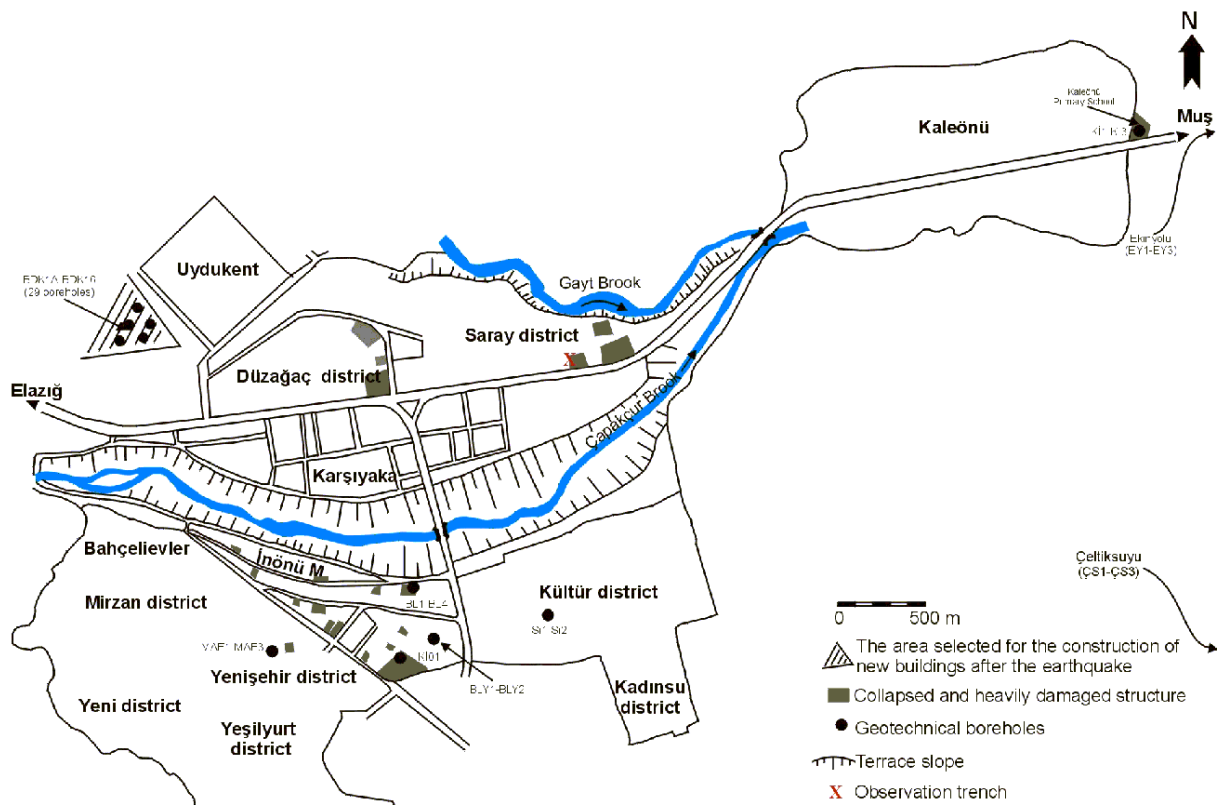


Figure 8.1: Locations of boreholes and trenches in Bingöl City

### 8.1 Local Site Conditions in Bingöl and Their Affects

The population of Bingöl City exhibited a rapid development following the 1971 Bingöl earthquake and reached up to about 70000 in recent years. During the 1971 earthquake, a large part of the city was founded on the bed of Çapakçur Brook. After this earthquake the city rapidly expanded onto the terraces at the north and south of this brook. Today the terraces, on which new Bingöl is founded, are divided by Gayt and Çapakçur Brooks (Figure 8.2), and

two parts of the city are connected by a bridge constructed on the Çapakçur Brook (Figure 10.5). The nearly flat-lying terraces about 40-45 m high have slope angles of  $45^{\circ}$ - $50^{\circ}$ . The information from the observation trenches and the data from the boreholes indicated that Bingöl City center is located on deep terrace deposits consisting of coarse gravel to boulder within stiff fine matrix (Figure 8.3).

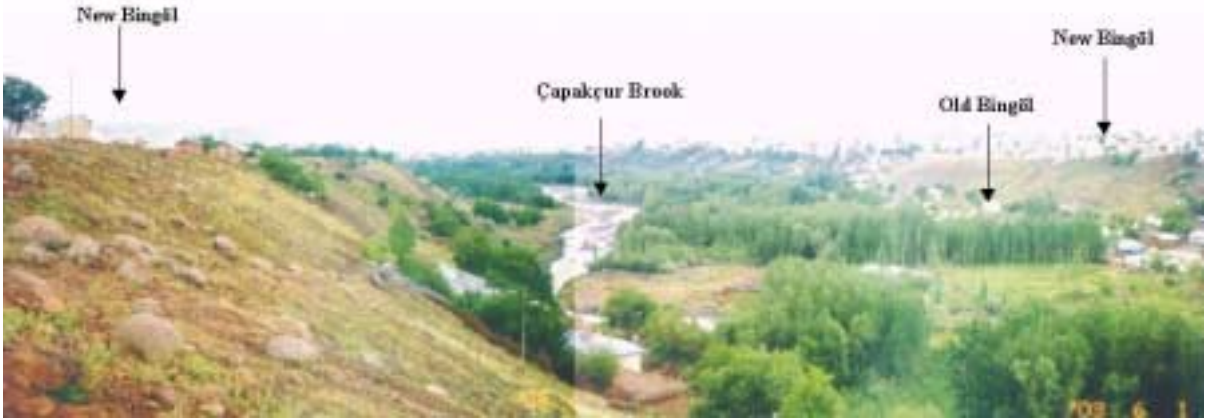
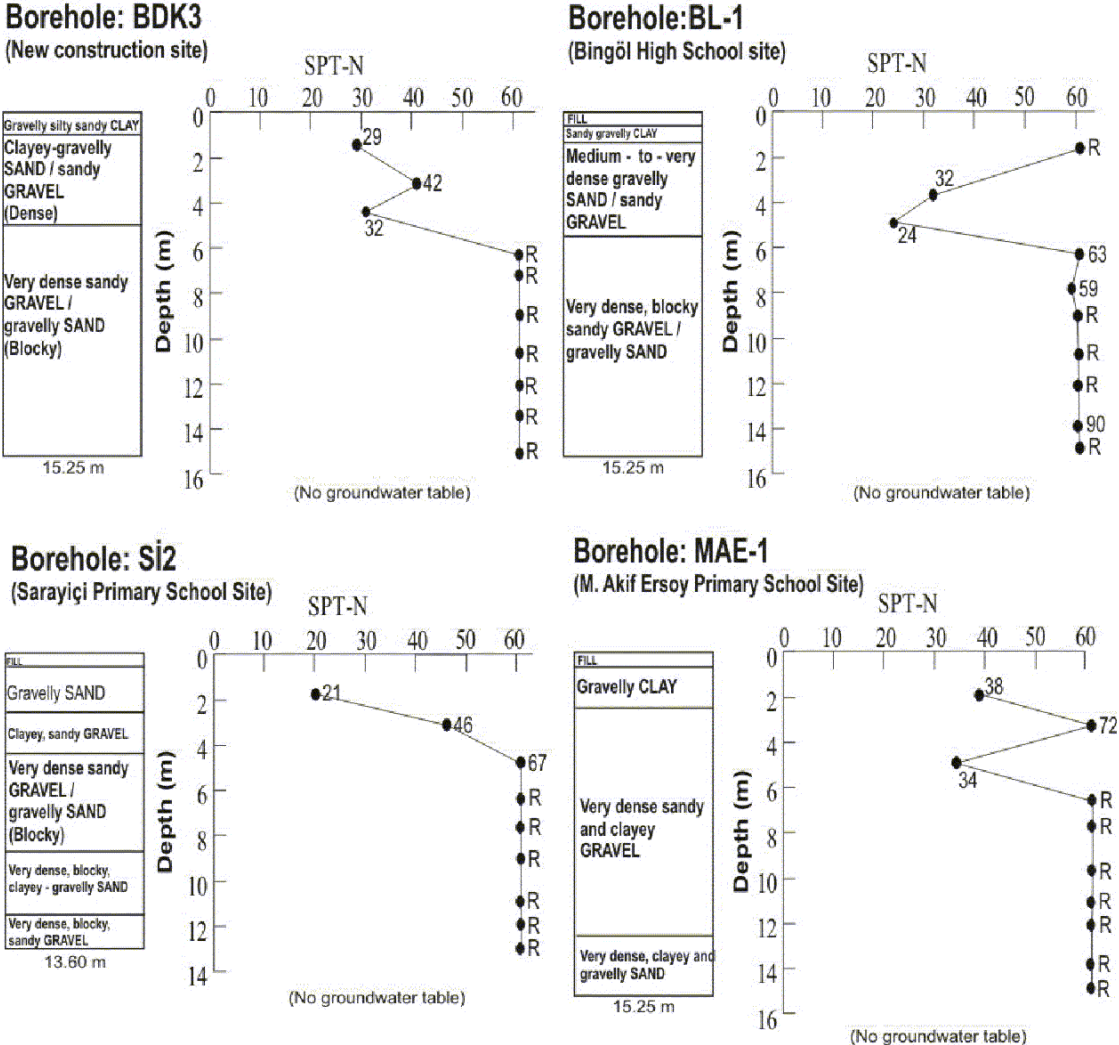


Figure 8.2: A view of Çapakçur brook and adjacent terraces



Figure 8.3: A view of soil condition in an observation trench

Some selected simplified borehole logs, which illustrate the variation of SPT-N values and soil type with depth in Bingöl city center, are shown in Figure 8.4. Generally residual soils and/or fill material 0.4-2.5 m thick overlays the terrace deposits, which are mainly composed of dark brown silty-gravelly sands and silty-sandy-blocky pebbles rounded and semi-rounded. These pebbles and blocks of various sizes are in volcanic origin. Based on the data provided from Yüksel Proje A.Ş. (2003a, b), these deposits mainly fall into GP-GM and GW-GM, and a few into SM and SC soil groups. SPT-N values from these deposits generally range between 20 and 35 from the surface to a depth of 5 m, while they are greater than 50 at depths greater than 5 m indicating very dense and stiff deposits. These features of the deposits are nearly identical throughout the city. Both the walls of observation trenches (Figure 8.3), and natural and man-made slopes (see Figure 8.2) in these stiff deposits seem to be highly stable even they have subjected to earthquake loads.



(R: Rejected; ie. N>50 between the interval of 15 - 30 cm of SPT test)

Figure 8.4: Logs of some boreholes in Bingöl City

No groundwater table was encountered through the boreholes and in observation trenches of about 4-5 m deep. It is reported by Yüksel Proje A.Ş. (2003a, b) that depth of the groundwater observed in water wells in the close vicinity was about 55-60 m. Deep groundwater table and subsurface ground conditions suggest that the terrace deposits underlying Bingöl city are not susceptible to liquefaction.

Based on the observations by the JSCE team, collapsed and heavily damaged buildings in Bingöl are also shown in Figure 8.1. These damages (Figure 8.5) are concentrated on the cliff sides of the terraces bounded by the Çapakçur and Gayıt Brooks. This situation suggests a possible amplification at the cliff sides due to topographical effects as presented in Chapter 7 and illustrated in Figure 8.6. These effects may also be responsible from the considerably high peak horizontal ground acceleration values measured at the Bingöl station, which is located close to the cliff side in Düzağaç district adjacent to the Gayıt Brook.



Figure 8.5: Collapsed or heavily damaged RC buildings nearby slope crest in Saray District

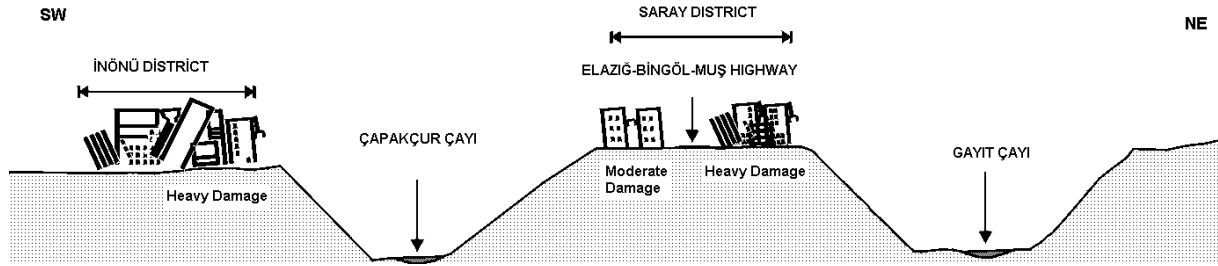


Figure 8.6: A topographic profile in NE-SW direction and its relation to damage state

Eastern and southeastern parts of the city center are located on relatively lower altitudes. These areas are formed by the Gayıt and Çapakçur Brooks (see Figure 8.2) and located in the Bingöl Plain. Kaleönü district of Bingöl city and Ekinyolu village at the east of Bingöl, and Çeltiksuyu village at its southeast are the settlements, where collapsed and heavily damaged cases were also observed. The terrace deposits with considerable amount of fines are also evident in the observation trenches and geotechnical boreholes drilled at these areas (Figure 8.7). However, the alluvial deposits fill the beds of these two brooks. In addition to dark brown silty-sandy gravels, the boreholes also penetrated into stiff sandy silt and silty sand layers. A typical section illustrating the soil layers and position of groundwater table at Çeltiksuyu Regional Primary Education School site, where the student dormitory and school building collapsed, is shown in Figure 8.8. Some selected simplified borehole logs summarizing site conditions are also given in Figure 8.9. Similar to those obtained in the terrace deposits at the central part of the city, very high SPT-N values were also recorded in the gravelly and blocky layers in this area. While the SPT-N values obtained in sandy, silty and clayey layers were between 12 and 48, and generally greater than 20, as can be seen from Figure 8.9. On the contrary to that in the city center, depth of the groundwater table at these lower altitude areas is very shallow. Based on the measurements by Yüksel Proje A.Ş. (2003c) it was at the surface (artesian condition) at Kaleönü Primary School site, and between 5.5 and 14.55 m at Çeltiksuyu Regional Primary Education School site in the southeast. Although the clay layers are impermeable, it is considered that the presence of silty sand layers and sandy nature of the clay layers permits circulation of the groundwater.

Although the three-story RC student dormitory and school building collapsed at the Çeltiksuyu site, a RC three-story building for teachers and a water tower about 25 m high located at a distance of 40 m from the collapsed buildings were not suffered any damage. By considering this very close distance between the collapsed and non-damaged structures, and

ground conditions in the observation trench and boreholes, it seems difficult to pronounce the contribution of the local ground conditions on the collapsed cases at this site.

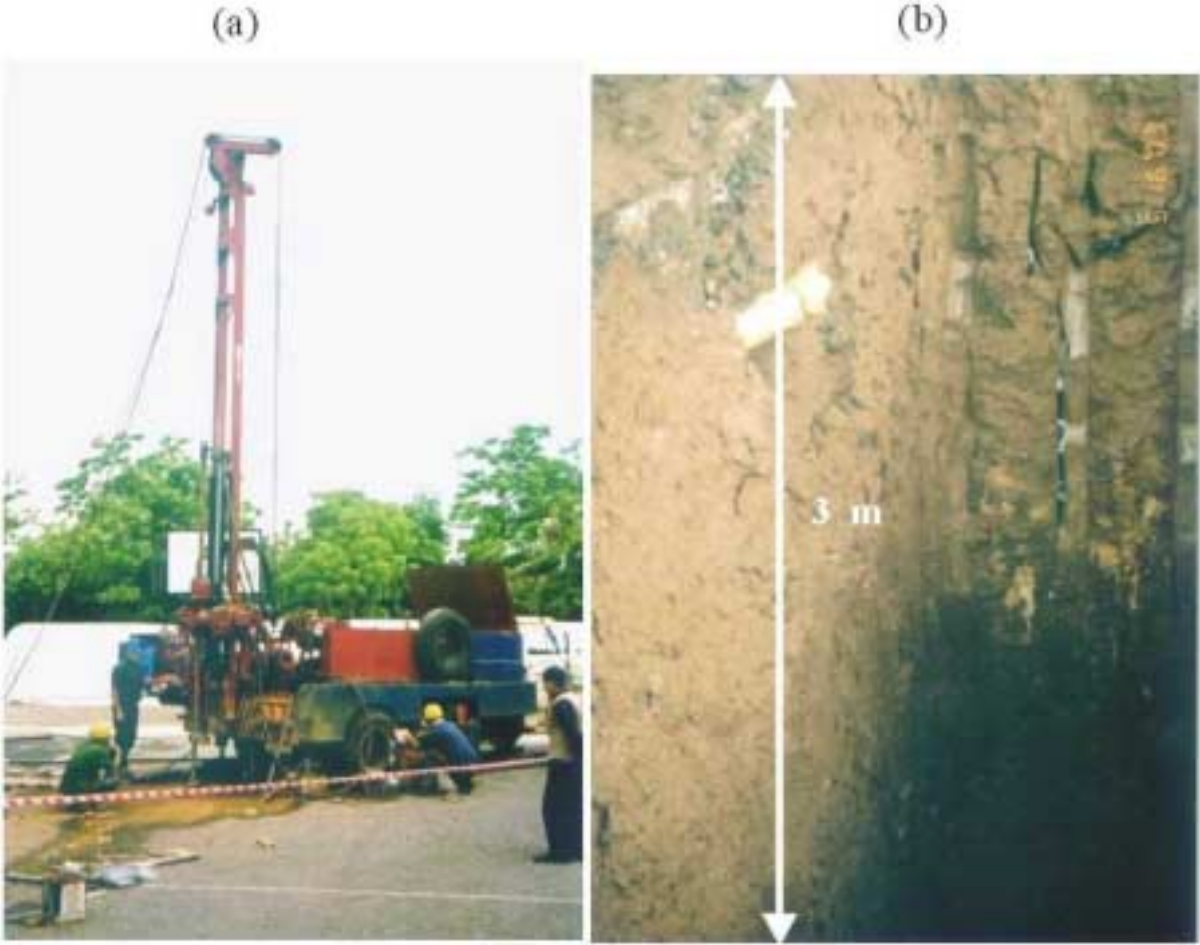


Figure 8.7: Views of some borehole drilling and observation trenches

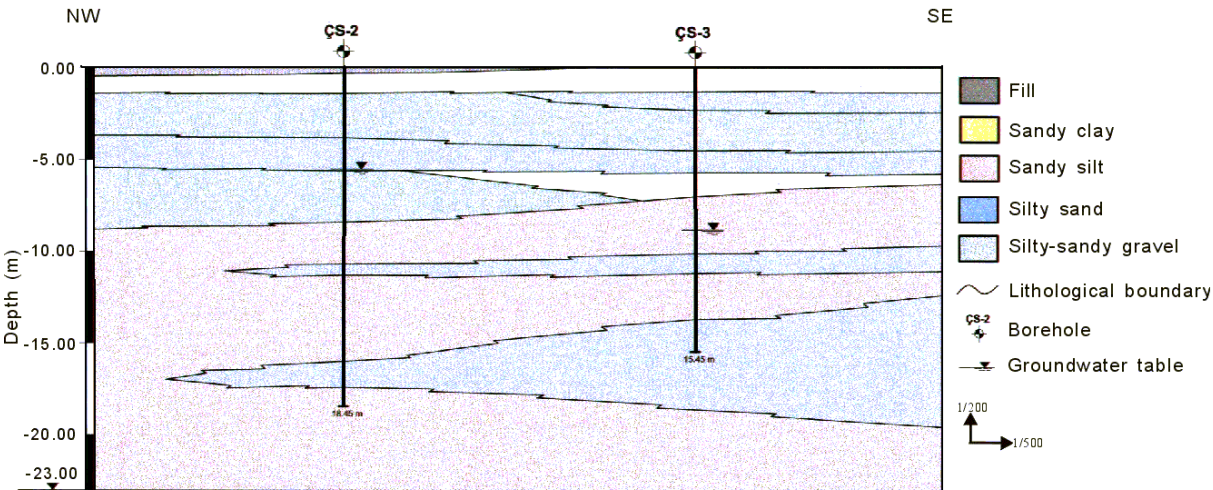
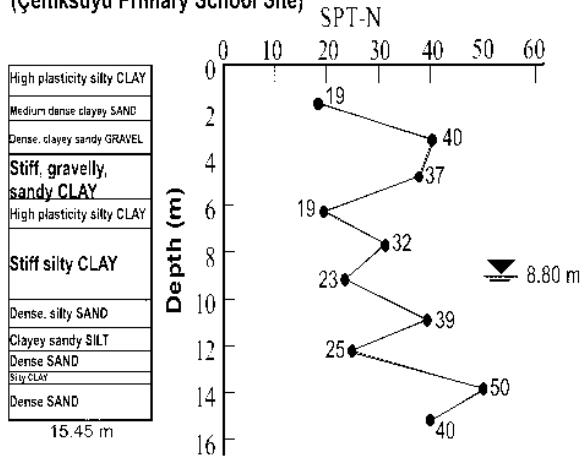


Figure 8.8: A simplified geologic cross-section in Çeltiksuyu

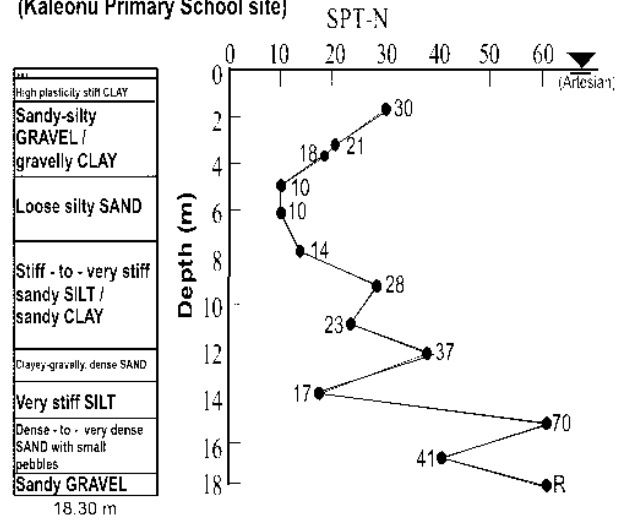
**Borehole: ÇS-03**

(Çeltiksuyu Primary School Site)



**Borehole: Kİ-3**

(Kaleönü Primary School site)



**Borehole: EY-1**

(Ekinyolu Primary School Site)

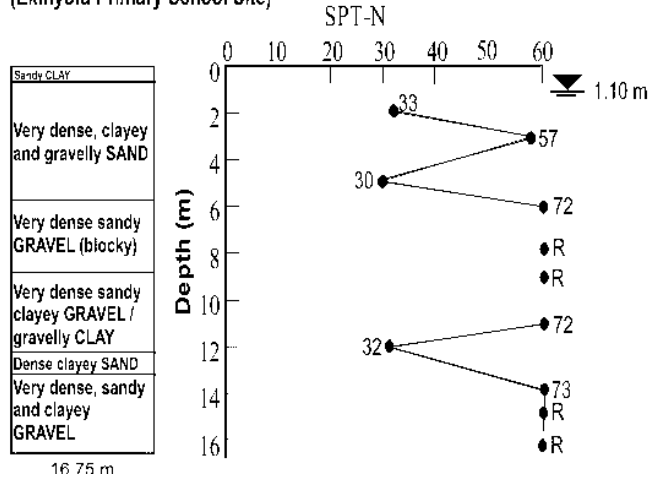


Figure 8.9: Logs of some boreholes at the sites of collapsed school buildings

Shear wave velocity ( $V_s$ ) of surface layers is a property widely used for empirical evaluation of site amplification. When  $V_s$  is not available for any site, SPT-N blow counts are used to estimate shear wave velocities (Technical Committee for Earthquake Geotechnical Engineering, 1999). Because no records of shear wave velocity data are available for the earthquake region, values of  $V_s$  were empirically estimated in this study. There are several empirical relations correlating SPT-N value and  $V_s$ . In this study, shear wave velocities for the surface layers were determined from the calculated equivalent SPT-N blow counts using the correlation between  $V_s$  and N given by Ohba and Trauma (1970),

$$V_s = 84N^{0.31} \tag{8.1}$$

The soil amplification ratios based on shear wave velocity were calculated using the relationship proposed by Midorikawa (1987).

$$A_k = 68V_s^{-0.6} \quad (8.2)$$

In the first stage, the borehole data from the center of Bingöl City was evaluated. Except the first 4-5 m from the surface in all boreholes, SPT-N values recorded in the terrace deposits were greater than 50 between 15-30 cm penetration interval of the SPT tests, and therefore, the test results from most of intervals were omitted. Due to this, the above-mentioned equations could not be used. However, by considering that the lower and upper limits of the SPT-N values ranged between 35 and 85 in between 0 and 5 m, amplification ratios ranging between 2 and 2.5 were calculated from the empirical equations. These preliminary assessments reveal that except the possible amplification due to topographic effect of the cliffs, amplification seems not to be a significant factor for the damage to buildings at the center of the city. Same empirical approach based on the data from the boreholes drilled on the flat-lying areas, where Kaleönü, Ekinyolu and Çeltiksuyu settlements are located, indicated amplification ratios were computed to be between 2.2 and 2.57, and generally 2.5.

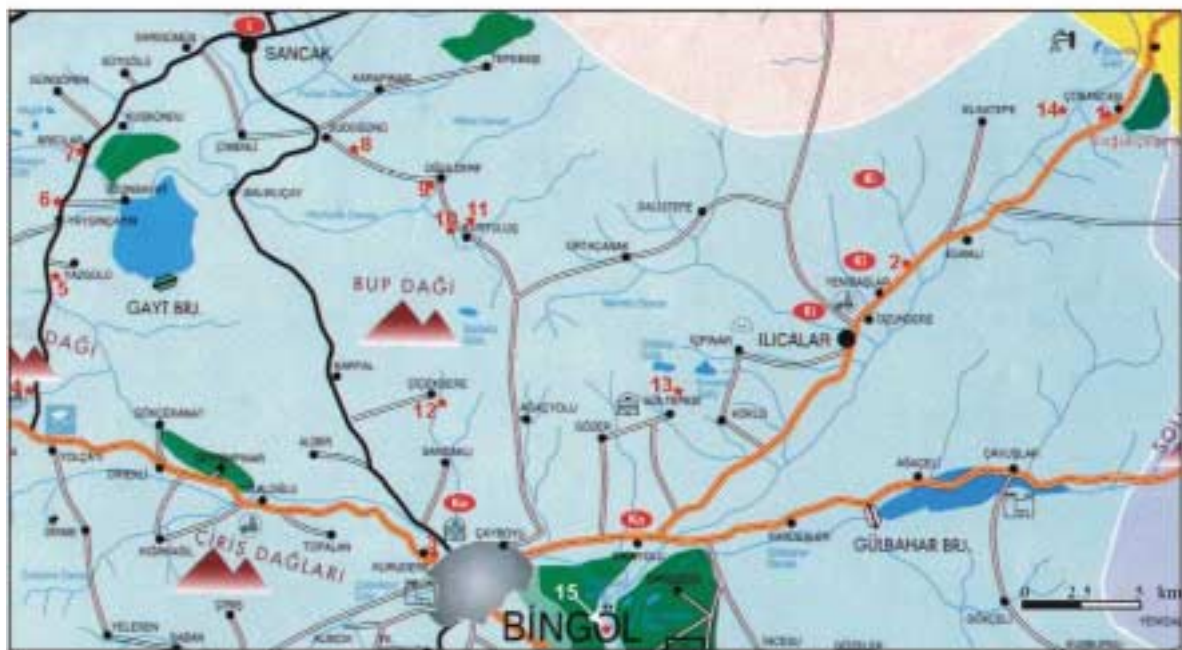
## **8.2 Site Effects at Rural Areas**

There are a number of villages in the epicentral area at the rural parts of Bingöl. These settlements are founded on volcanic rocks in various degrees of weathering. In these rural areas constructions are single story buildings of stone masonry. Due to short investigation period of the JSCE team and no boring data at these settlements, any assessment on the site effects could not be possible. However, at Çimenli village (Figure 13.5(d)) which is founded both on a small hill at the north and a flat-lying area at the south, the houses with heavy roofs on the hill side heavily damaged and/or collapsed having, while the others suffered to light damage. Based on the information from the villagers, a similar damage distribution was observed in this village during the 1971 Bingöl earthquake. This situation indicates either the possible contribution of topographical effects or the effect of their heavy roofs on the observed damage.

## **8.3 Seismically-triggered Landslides**

A number of seismically triggered landslides were observed in the epicentral area. These landslides occurred in the form of rotational or shallow-seated planar failures, rock falls and

mudflows and their locations are shown in Figure 8.10. Depth and type of the landslides were primarily controlled by the degree of weathering. Rotational or shallow-seated planar failures and flow type failures have occurred in residual soils originated from the volcanic rocks, while rock falls were from jointed and fresh-to-slightly weathered volcanics forming steep slopes. The landslides were generally concentrated close to the epicenter of the earthquake. It is also noted that heavy rains in the region within two weeks before the earthquake are considered to contribute to softening of the materials before they were subjected to dynamic loads. Main features of the landslides are briefly given in the following paragraphs.



1,2,3,5,9: Rotational slide; 4,7,10,12,13: Rock fall; 6,8: Liquefaction and lateral spreading;1,14,8: Flow; 15: Liquefaction

Figure 8.10: Locations of geotechnical failures

### 8.3.1 Rotational or shallow-seated planar failures

***Soğukçeşme landslide:*** This landslide occurred on the Bingöl-Karlıova road at the NE of Bingöl in very thick weathering products of volcanic rich in silt sized material (Location 1 in Figure 8.10). This rotational failure, which occurred on the SE bank of the Göynük Brook, was transformed into flow type instability extending about 80 m towards west (Figure 8.11a). The failed slope 25m high has an inclination of about  $30^{\circ}$ , and height of the scarp is 7 m. The failure also slightly effected the asphalt pavement of the road as seen in Figure 8.11b.

**Herdere slide:** This small local slide was observed at Herdere location between Ilıca and Soğukçeşme on the SW cut of the Bingöl-Karlıova road (Location 2 in Figure 8.10). The failed material is similar to that observed at Soğukçeşme slide (Figure 8.12).



Figure 8.11: Landslide at Soğukçeşme



Figure 8.12: Landslide at Herdere

**Bingöl slide:** A local slide on the southern cut of the Bingöl-Elazığ road occurred at the western end of Bingöl (Location 3 in Figure 8.10). The sliding material is composed of terrace deposits involving relatively high amount fines. It is a 10m high slope with an inclination of  $65^{\circ}$  (Figure 8.13).

**Yazgülü slide:** This slide occurred on the road cut at the south of Yazgülü village (Location 5 in Figure 8.12). The slope forming material was a residual soil originated from volcanic rocks (Figure 8.14), and the movement was towards S35W. However, stable adjacent slopes, which are composed of less weathered material, have  $40^{\circ}$  inclinations.

**Oğuldere slide:** This slide occurred near Oğuldere village and a large volume of weathered volcanic rock moved towards a stream (north), which flows parallel to the toe of the slope (Location 9 in Figure 8.10, and Figure 8.15). It is about 30-35 m high slope with an inclination of  $45^{\circ}$ .



Figure 8.13: Bingöl slope failure



Figure 8.14: Yazgülü slope failure



Figure 8.15: Oğuldere slope failure

### 8.3.2 Mudflows

A long mudflow occurred in Kurtuluş village on a hill slope at the north of the village (Location 11 in Figure 8.10). The material, which was flowed down hundreds of meters, is weathered tuff. The weathered material, which probably become fully saturated before the earthquake due to heavy rains, flowed through a long wedge resulted from two intersecting relict discontinuities and the along the low-angle topography towards lower elevations where the movement has stopped, as seen in Figure 8.16. The slope was 50 m high and has an inclination of  $45^{\circ}$ - $50^{\circ}$ , and direction of flow was towards S30W.

As mentioned in the previous section, a mudflow, which followed a circular failure, occurred at Soğukçeşme (Figure 8.11). Another mudflow was observed in the west of this slide on the eastern bank of the Göynük Brook (Location 14 in Figure 8.10). It was a small-scale mudflow occurred in weathered volcanics along a steep slope.



Figure 8.16: Kurtuluş slope failure and mudflow

### 8.3.3 Rock falls

A number of rock falls were observed at some villages and along the roads connecting the settlements to each other at the northern part of Bingöl. However, all these instabilities occurred at rural areas, and therefore, did not cause any loss of life and damage to structures. Some small volume rock falls were documented at a location called Germik Komu between Yolçatı and Yazgülü villages (Location 4 in Figure 8.10, and Figure 8.17a). Rock blocks from a jointed basaltic rock mass fallen down towards the road (to north). It is about a 15m high slope with a dip angle of  $50^{\circ}$ , and the main joint sets dip towards the road.

A large basaltic block approximately 1.70 m high and 1 m wide fallen down from the road cut and stopped on the road at the northern exit of Arıclar village (Location 7 in Figure 8.10 and Figure 8.17b, c). Inclination of the slope in 6 m high was  $35^{\circ}$  and the movement direction of the block was S42E. A huge rock block about 3 m in diameter fallen down (Figure 8.17d) from a steep cliff (Location 10 in Figure 8.10) at the NW entrance of Kurtuluş village.



Figure 8.17: Rock falls

Another place, where rock falls were observed, is Göltepesi village located on the hills at NE of Bingöl (Location 13 in Figure 8.10). The slope surrounding the village from its north is composed of partly weathered blocky andesite, and has an inclination of  $40^{\circ}$ - $50^{\circ}$  towards south. Some local falls of rock blocks with dimensions approximately (90x35x60) cm were observed (Figure 8.18a). Displacement of these rock blocks from their original position was estimated about 2.5-3 m. In addition to rock falls, some cracks trending in E-W direction were evident at the crest of the slope. Their persistence ranged between 5 and 10 m and separation between the walls of these cracks was about 10 cm (Figure 8.18b). These cracks were tension cracks indicating a slope movement towards south. However, they are highly local cracks and the movement could not be transformed into a catastrophic failure.



Figure 8.18: Rock falls behind Göktepesi

## 8.4 Liquefaction-induced Ground Deformations

Liquefaction induced ground deformations in the form of lateral spreading and sand boiling were observed at three locations, near Yaygınçayır village, Hanoçayırı at the epicentral area and at a location between Bingöl-Genç road and Göynük Brook at SW of Bingöl (Locations 6, 8 and 15 in Figure 8.10). Since these deformations occurred in rural areas, they didn't cause any structural damage.

### 8.4.1 Lateral spread at Yaygınçayır village

The first place, where ground deformations resembling a lateral spreading were observed by the JSCE team, was at the northern exit of Yaygınçayır village (Location 5 in Figure 8.10). At

this location, where Uğurboğa Stream 5 m wide flows from west to east, three zones of lateral spreading were identified on the northern bank of the stream (Figure 8.19a). The failure pattern and a sand accumulation very similar to a sand boil on the southern bank of the stream (Figure 8.19b) suggest that this failure can probably be due to a liquefaction-induced lateral spreading. The inclination of the failed stream bank was about  $10^{\circ}$ - $15^{\circ}$ . The displacements due to lateral spreading in these zones were measured as 16.5, 21 and 30 cm, respectively. Width of the zone of ground deformation was 60 m and the sliding material was a dark brown, low plasticity silt-clay-sand mixture.



Figure 8.19: Lateral spread nearby Yaygınçayır village

#### 8.4.2 Lateral spreading at Hanoçayırı

The second but a very significant lateral spreading occurred at a location called Hanoçayırı. This locality is near the road between Sudüğünü and Oğuldere villages and is very close to the epicenter of the earthquake (Location 8 in Figure 8.10). It is surrounded by topographical undulations consisting of white-to-beige colored tuffs. Silt and sand sized surficial material, which is the weathering product of the tuffs, cover the lower altitudes. The presence of this shallow-seated silt and sand sized non-plastic material and shallow groundwater table, which was evident during the observations at water well very close to the failure, resulted in a highly susceptible environment to liquefaction. Inclination of the ground where was about  $3^{\circ}$ - $4^{\circ}$ , where liquefaction-induced lateral spreading followed by a flow occurred (Figure 8.20). Traceable sand accumulations observed near the eastern flank of the failure (Figure 8.21a) and in the lateral spreading area were evaluated as the indicator of liquefaction. The loose material, which was also saturated due to heavy rains before the earthquake, flowed down in S55W direction about 300 m, and then directed towards SE. The total length, width and

maximum depth of the flow was approximately 600 m, 35 m, and 3 m, respectively. Evident set of ground deformations, which were resulted in 30-35 cm vertical drops (Figure 8.21d) and separations of 10-20 cm in the ground behind the crest and near the flanks of this failure, was observed (Figure 8.21b and c). A total lateral displacement of about 90cm was measured at the crest region of the failure.



Figure 8.20: A view of lateral spreading at Hanoçayırı



Figure8.21: Some views of lateral spreading phenomenon at Hanoçayırı

Three specimens from the ejected and flowed material were collected and employed to determine their specific gravity, grain size distribution and shear strength. In addition, two shallow-seated geotechnical boreholes were drilled a few meters behind the crest and near the western flank of the failure (Figures 8.22) in June 2003 to assess the subsurface conditions, to obtain samples for laboratory tests, and to perform back analysis of the liquefaction.



Figure 8.22: Borehole drilling at Hanoçayırı

Laboratory testing on the samples from ejected and flowed materials, which are described as sand and silty sand in the field, consisted of specific gravity, grain size distribution and shear strength. Because a long time passed after the failure during the site observations, water content determinations could not be carried out. Specific gravity of two ejected and flowed soil samples was obtained as 2.5 and 2.4, respectively. Sieve analyses were conducted on 3 samples, and grain size distribution curves of each sample were plotted into grain size distribution of liquefiable soil proposed by Japan Port and Harbor Research Institute (1997) in Figure 8.23. It is evident from this figure that sand size material with fines content of 7-12% is dominant (SP group soil) in the liquefied soil and flowed surficial material involves greater amount of fines (SM group soil). However, all the samples fall into the limits designated by most liquefiable. Static shear strength of the samples was determined employing motorized direct/residual soil shear test device. Totally 3 specimens from each sample were prepared to fit the shear box. All tests were run at a strain of 0.25 mm/min. Failure envelopes of all samples (Figure 8.24) show a consistency indicating that the samples are cohesionless soils with an internal friction angle ranging between  $42^{\circ}$  and  $44.5^{\circ}$ .

For the petrographical description of the liquefied material the XRD diffractogram of one of the three samples from the site was obtained at X-Ray Micro Analysis Laboratory of the Geological Engineering Department at Hacettepe University using a Philips PW-1140 model diffractometer with a goniometer speed of  $2^{\circ}/\text{min}$ . The XRD pattern for the sample is depicted in Figure 8.25. The whole sample mineralogy indicated that the sample mainly comprised of feldspar, and lesser amounts of quartz and calcite. This composition and site observations revealed that the liquefied and spreaded material was a weathering product of the tuffs surrounding the Hanoçayırı location.

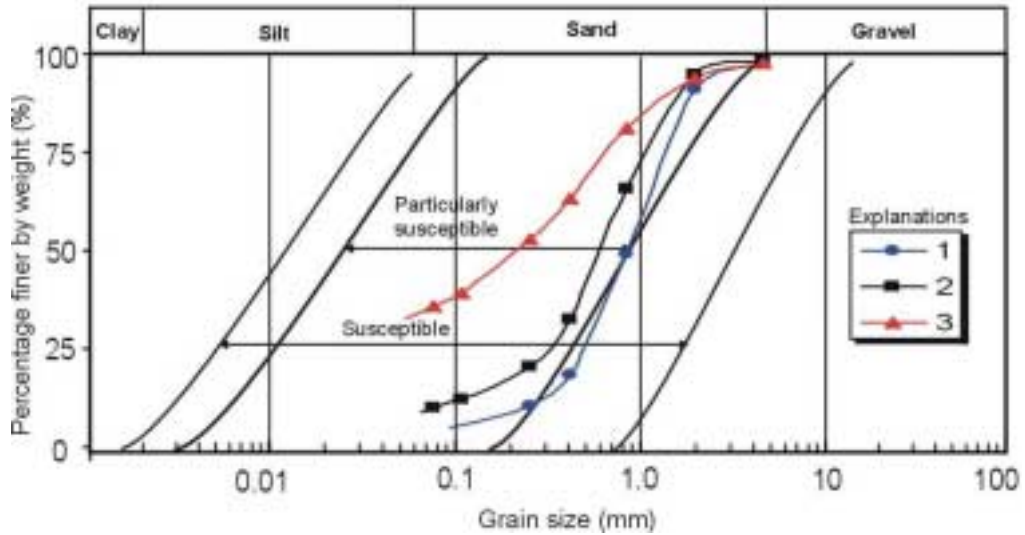


Figure 8.23: Grain size distributions of soil samples at Hanoçayırı

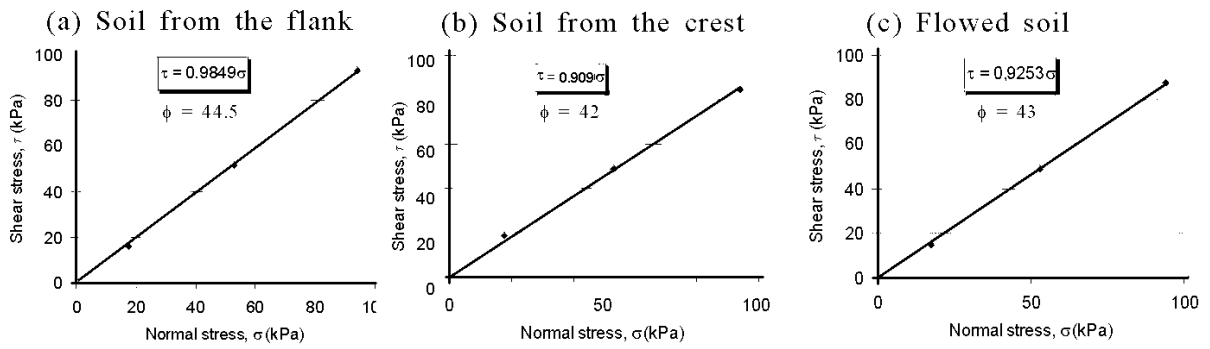


Figure 8.24: Shear strength envelopes of soil samples at Hanoçayırı

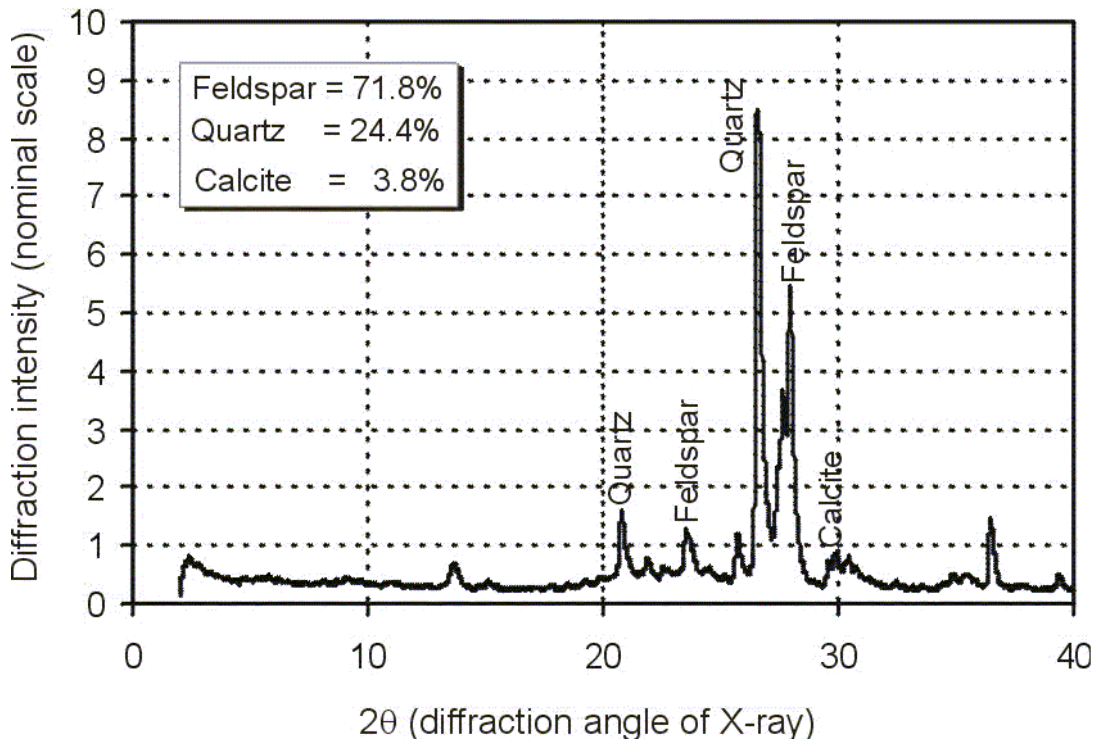


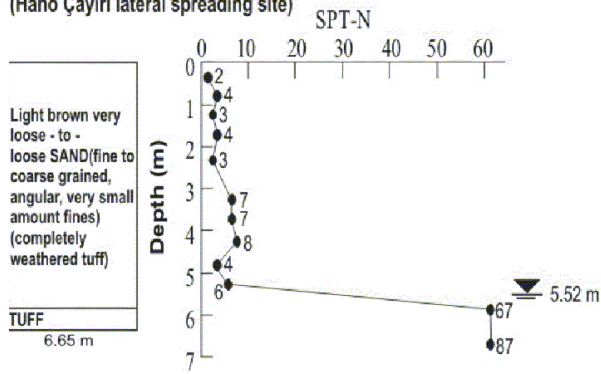
Figure 8.25: XRD pattern of the soil sample

Two boreholes (H1 and H2), 6.65 m and 5.25 m deep, respectively, were drilled at Hanoçayırı. The distance between the boreholes is about 100 m. Simplified logs of these boreholes are depicted in Figure 26. It is evident from Figure 26 that the uppermost level of the sequence approximately between 0 and 5.5 m consists of light brown-to-beige, very loose-to-loose sand sized material derived from the tuffs (Figure 27). This material is moist-wet, fine-to-coarse grained, and includes angular-subangular grains with some fines. SPT tests were carried out at every 50 cm interval throughout both boreholes. In this material, very low SPT-N values, which ranged between 2 and 8 and generally between 2-4 near to the surface, indicated a very loose state suitable for liquefaction. The bedrock (tuff) lies at about 5 m from the surface. Depth of the groundwater table at the location of borehole H1 was measured as 5.5 m, while it was at 2.25 m below the surface in borehole H2. If the relative elevations of the boreholes and topographical inclination ( $3^{\circ}$ ) are considered it can be concluded that position of the groundwater table was nearly parallel to the surface at the time of drilling. However, it is expected that depth of the groundwater table could have been very shallow during the earthquake than that of measured from boreholes, probably because of heavy rains occurred before the earthquake.

The laboratory soil classification tests from SPT samples suggest that the loose and shallow seated material overlying the bedrock falls into SM group which is defined as silty sand. This material also includes silt and clay sized fine grains in the range of 24-43% with ignorable amounts of gravel, and shows a close similarity to those of the materials collected from the surface (see Figure 8.28). Figure 8.27 shows the grain size distribution range of the SPT samples from both boreholes and they fall into the limits designated by most liquefiable. Shallow seated groundwater, and its grain size characteristics and loose state make this surficial material highly susceptible to liquefaction. Back analysis of the liquefaction was carried out to estimate the minimum value of the horizontal ground acceleration ( $a_{\max}$ ) which might have caused to initiate liquefaction. For the purpose, the data from the boreholes H1 and H2 was used. Depth of the groundwater table was taken 2.25 m for borehole H2 as measured, while it was assumed 3 m for the location of borehole H1 by considering the heavy rains before the earthquake. The method based on the field performance data (Youd et al., 2001) was employed as a means of evaluating acceleration by back analysis approach. Necessary corrections for the SPT-N, energy ratio and overburden pressure were all considered and normalized SPT-N values,  $(N_1)_{60}$ , were calculated.

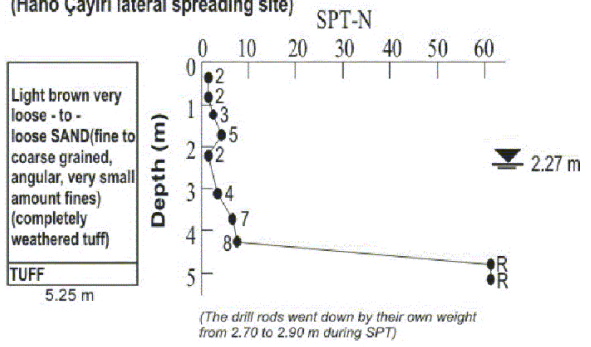
**Borehole: H-1**

(Hano Çayırı lateral spreading site)



**Borehole: H-2**

(Hano Çayırı lateral spreading site)



(R: Rejected; ie. N>50 between the interval of 15-30 cm of SPT test)

Figure 8.26: Simplified borehole logs at Hanoçayırı

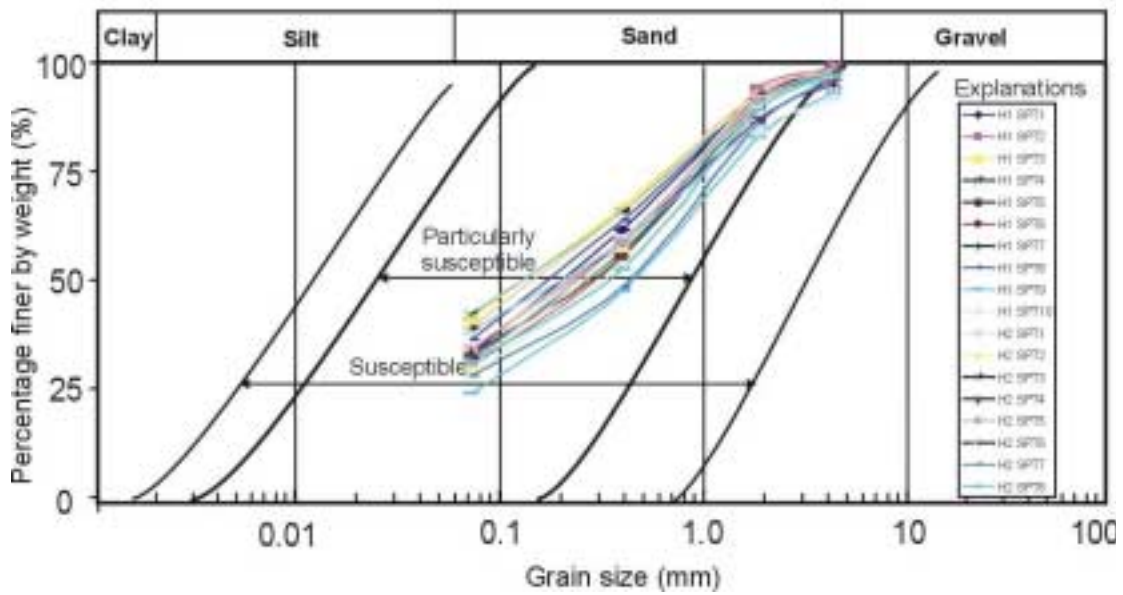


Figure 8.27: Grain size distributions of borehole samples at Hanoçayırı



Figure 8.28: A view of a borehole soil sample at Hanoçayırı

It is evident from Table 8.1 that depending on the number of blows and fines content,  $a_{max}$  values ranging between 166 gal and 263 gal were calculated and they seem to be necessary for initiating the liquefaction at this site. It, however, should be kept in mind that these back-calculated  $a_{max}$  values are the minimum values to trigger liquefaction. If the very close proximity of Hanoçayırı to the hypocenter of the earthquake is taken into account, an  $a_{max}$  value, which is probably greater than those back-calculated in Table 8.1, can be considered to act at Hanoçayırı and its close vicinity during the earthquake. Based on the above assessments, it can be concluded that liquefaction has occurred in a saturated silty sand, which is a surficial weathering product of tuff with a thickness of about 5 m. This liquefied material laterally spreaded and then flowed with the contribution of its very high moisture content.

Table 8.1 Back analysis results of the liquefaction at Hanoçayırı.

(a) Borehole: H1 (GWT: 3 m)					
Depth (m)	SPT-N	$(N_1)_{60}$	Soil Class	FC (%)	$a_{max}$ (gal)
0.3	2	1.91	SM	34	
0.8	4	3.83	SM	31	
1.3	3	2.87	SM	42	
1.8	4	3.65	SM	43	NE
2.3	3	2.59	SM	35	232
3.3	7	5.84	SM	34	263
3.8	7	5.60	SM	33	243
4.3	8	6.54	SM	37	255
4.8	4	3.15	SM	25	166
5.3	6	4.57	SM	29	193
(b) Borehole : H1 (GWT: 2.25 m)					
0.3	2	1.91	SM	35	
0.8	2	1.91	SM	31	
1.3	3	2.87	SM	39	
1.8	5	4.57	SM	35	NE
2.3	2	1.73	SM	32	207
3.2	4	3.37	SM	29	205
3.7	7	5.64	SM	32	243
4.2	8	6.59	SM	35	257

NE: Not evaluated, because the layer is above the groundwater table.

GWT: Depth of groundwater table.

In this study, a comparison was also made between the observed ground deformations at Hanoçayırı and the results from a prediction equation suggested by Hamada et al. (1986). These investigators predict the amplitude of horizontal ground deformation only in terms of slope and thickness of liquefied layer:

$$D = 0.75H^{0.5}\theta^{0.33} \quad (8.3)$$

Where  $D$  is the horizontal displacement (m),  $\theta$  is the slope (%) of ground surface or base of liquefied soil and  $H$  is the thickness (m) of saturated zone below the ground surface. By considering that the thickness of the saturated zone below the ground surface in borehole H2 is 2 m and  $\theta$  is 1%, the magnitude of the lateral displacement was estimated as 1.05 from the above equation. This predicted value is consistent with that measured at the site (90 cm).

### 8.4.3 Liquefaction at the Bingöl Plain

Liquefaction was also observed at Bingöl Plain according to the information provided by N. Bartakuçin who is the Manager of TEDAŞ at Bingöl. As can be seen from Figure 8.10, it occurred at a location between Göynük Brook and Bingöl-Genç road in a farm field. Although the JSCE team and Mr. Bartakuçin spend some effort to find this location one month after the earthquake, it was not possible to find it as it was disturbed by the villagers for farming. However, the photograph showing this sand boiling taken by Mr. Bartakuçin is shown in Figure 8.29. From this figure, sand boiling and sand accumulation are evident, and groundwater table seems to be very shallow. It is also noted that the alluvial sediments carried by Göynük Brook cover this area.



Figure 8.29: Liquefaction in Bingöl Plain (photo by N. Bartakuçin)

## 9 LIFELINES

The damages to lifelines are categorised into four groups and described in the following subsections.

### 9.1 Electricity

The electricity of Turkey is produced and distributed to main transformation stations by TEAŞ. From these main transformation stations, the electricity is distributed to the cities and industrial facilities by TEDAŞ. These two companies are owned by the state. Figure 9.1 shows the electricity system of Turkey and the functions of the electricity companies.

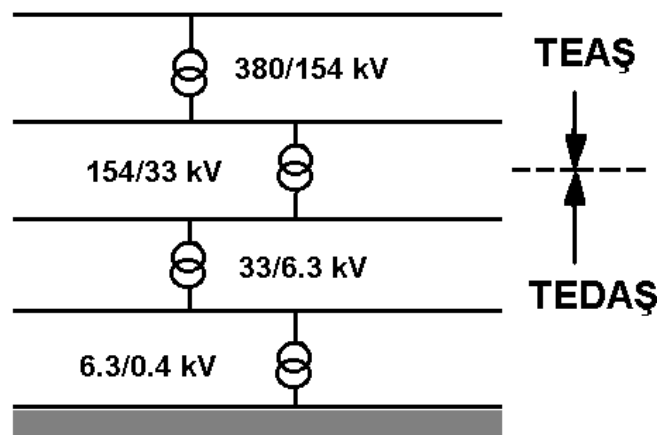


Figure 9.1: Electricity system of Turkey and the functions of TEAŞ and TEDAŞ

The nearest power stations to the epicenter of the Earthquake were Özlüce, Keban and Karakaya hydro-electric power plants (Figure 9.2). Although acceleration records at these power plants are not available, no damage to power plants was reported so far. Since all these power plants were founded on rock, the amplitude of maximum acceleration could be small as compared with those on alluvial deposits.

During the earthquake, the region lost power shortly after the earthquake since it is customary to automatically shut off the power as soon as a large earthquake happens.

After some preliminary checks on the location of the earthquake, the power was gradually supplied to the region in order to prevent fires or accidents due to short circuits, which could be caused by the collapsed or heavily damaged structures.

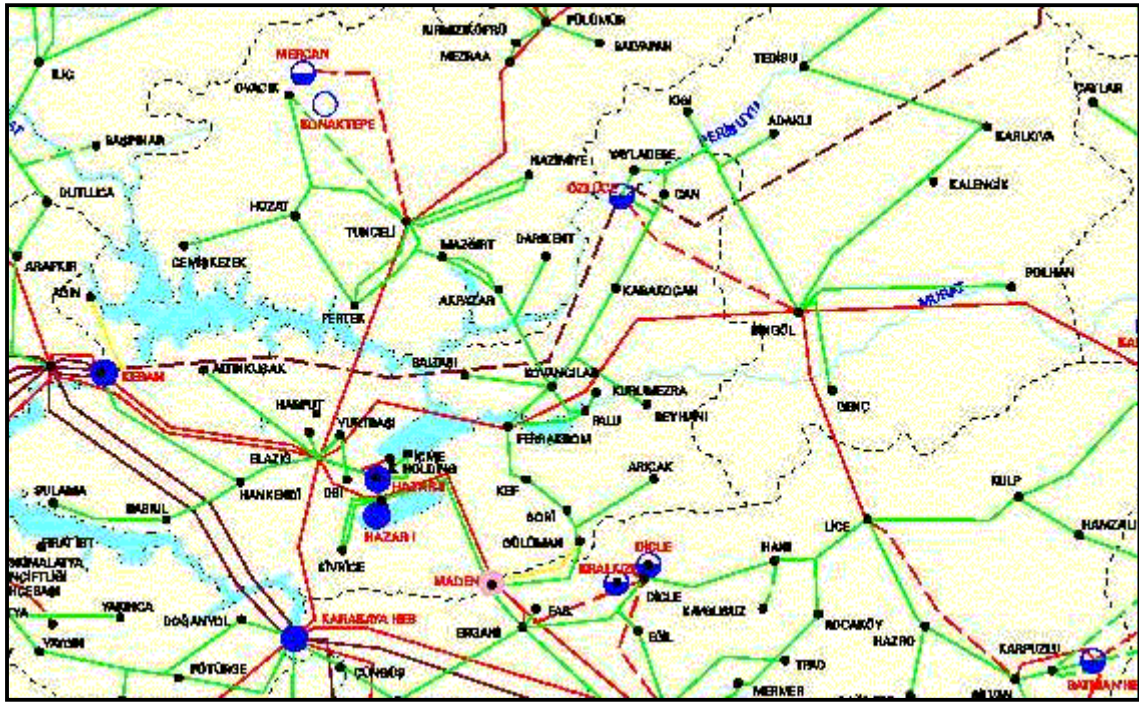


Figure 9.2: Electric transmission and distribution network in Bingöl region

There was one main sub-station, namely, Bingöl, which reduce the voltage from 154.0 kV to 33 kV (Figure 9.3). During this earthquake, the sub-station was not damaged, although some sliding and rocking of three transformers of Bingöl sub-station of TEDAŞ occurred because of shaking (Figure 9.4). However, the effects were minimal without disturbing their functions. Some elevated transformers on pylons in the towns and cities were displaced from their locations. Poles and pylons of the electricity distribution system in Bingöl and nearby towns and villages were not damaged due to ground shaking. The electricity was back 4 hours after the earthquake. The electricity was first supplied to the state hospital. At 9AM, the other two hospitals and semi-underground water reservoirs were supplied with electricity. Due to sliding of transformers at water reservoirs, they can not be in operation by 2 PM on May 1.



Figure 9.3: Non-damaged Bingöl sub-station



Figure 9.4 Slightly displaced transformer

## **9.2 Water Supply Systems**

The municipality of Bingöl runs the water supply system. The water is obtained from aquifers and it is pumped to buried reservoirs on the most suitable and highest hills in order to facilitate a smooth and economic water supply with the use of gravity after purification. No damage to the wells, pipes and pumps of the water supply systems of these two cities was reported. The water supply system was slightly damaged at some locations in Bingöl City. The main water pipes have a 100-300 mm diameter and are made of ductile iron and asbestos. Particularly asbestos pipes were damaged by splitting as they are brittle.

## **9.3 Sewage Systems**

The diameters of sewage pipes are 100 mm and 400 mm beneath boulevards and streets, respectively. The sewage system of Bingöl was almost non-damaged. Nevertheless the damage was observed at locations where the sewage pipes were connected to buildings.

## **9.4 Telecommunication System**

The telecommunication system in Turkey is run by the TÜRK-TELEKOM. During the earthquake, the main building of the TÜRK-TELEKOM was slightly damaged in spite of its poor construction quality. However, the relay towers of the system were almost non-damaged. The generator anchored to foundation was non-damaged and it was in operation as soon as the electricity supply was cut. The telephone system was almost uninterrupted except the heavily damaged areas. The telephone service was well-functioning and no congestion of phones to the region was observed. Additional first aid telephone lines were set up by the TÜRK-TELEKOM and were free of charge soon after the earthquake, including all public telephones. Figure 9.5 shows some views of the equipments of facilities of the telecommunication station.



(a) Building



(b) Displaced sand bucket (1<sup>st</sup> floor)



(c) Anchored generator



(d) Battery racks



(e) Tilted racks



(f) Relay tower

Figure 9.5: Views of equipments and facilities at Bingöl Telecommunication station

## 10 TRANSPORTATION FACILITIES

### 10.1 Roadways

The main highways in the earthquake stricken region are Erzurum-Bingöl-Diyarbakır (D950) and Elazığ-Bingöl-Muş (D300). The small towns and villages of Bingöl province are connected to Bingöl through paved roadways. None of highways was damaged by the earthquake except some damage by slope failures or embankment settlements. Since roadways and highways are mostly built on natural ground directly, the damage to roadways was quite limited. The most severe roadway damage was observed nearby Çobantaşı village on Bingöl-Erzurum segment of D950 State Highway (Figure 10.1). The slope was consisted of highly weathered volcanic deposits and it failed in a rotational mode of failure. The slope failure on the roadway nearby Yazgüllu village between Yolçatı and Sancak caused the heaving of its asphalt pavement (Figure 10.2). The rockfalls at Arıcılar on the Yolçatı-Sancak roadway and Kurtuluş village between Sancak-Bingöl are worthwhile (Figure 10.3). At both sides spheroidal basaltic rock blocks were toppled on the roadways. While the block nearby Arıcılar stopped on the roadway due to a small vertical drop of 3-4m, the failed block nearby Kurtuluş village was quite huge and disintegrated into several fragments during tumbling over the slope. The vertical drop was more than 30m.

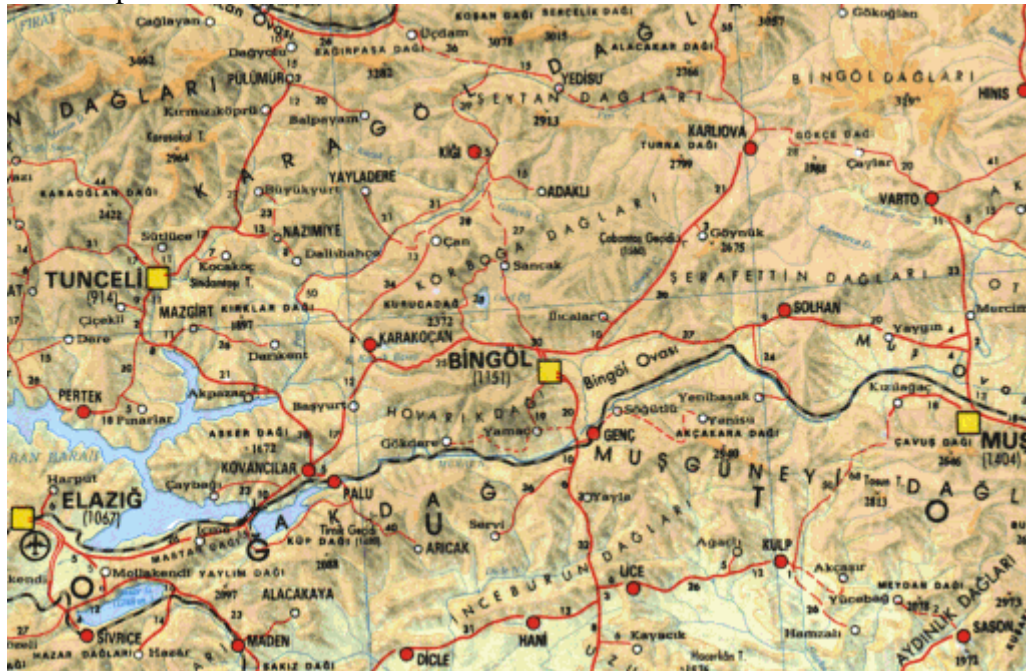


Figure 10.1: Main highways and railways in Bingöl province and its close vicinity



Figure 10.2: Damaged roadway nearby Yazgülü village on Yolçatı-Sancak Roadway



(a) Arıcılar village



(b) Kurtuluş village

Figure 10.3: Fallen rock blocks on roadways

## 10.2 Railways

The railway between Ankara and Tatvan of TCDD (The State Railway Authority of Turkish Republic) passes through the southern part of Bingöl province, which roughly follows the valley of Murat river. There is a railway station at Genç town, which is about 20km the south of Bingöl City. No damage to the railways or railway station by this earthquake was reported. However, the railway bridge spanning over Murat River was slightly damaged in the 1971 earthquake.

## 10.3 Bridges

The highway bridges over Gayıt, Çapakçur and Göynük Suyu brooks nearby Bingöl City and a highway and railway bridge over Keban dam lake at Gülüşkür and small bridges in the epicentral area were investigated. The RC three-span bridge (Axis is EW) over Gayıt brook (Bingöl-Erzurum Highway) was not damaged (Figure 10.4). The bridge is cast in-place and girders are simply supported. Another RC two span bridge (Axis NS) at the north of Bingöl City was also non-damaged.

The RC two span bridge (Axis is NS) over Çapakçur brook in Bingöl City was also non-damaged. Nevertheless, some flaking of piers and sliding of embankment cover panels at southern sides of the bridge was observed (Figure 10.5).

The RC five span bridge (Axis NS) over Göynük brook was slightly damaged. This bridge is about 60m long and its structural mechanics model is Gerber-type as shown in Figure 10.6. Some flaking of piers and sliding of Gerber-type girder were observed. The offset sliding of the girder at the southern part of the bridge was about 10cm. Similar damage to this bridge was also observed in the 1971 earthquake (see the report by Aktan et al. 1972).

The highway and railway bridges over Keban dam lake at Gülüşkür were non-damaged (Figure 10.7). The RC two span bridge at Çimenli village and small bridges nearby Arıcılar and Punan brook between Sancak and Sudüğünü in the epicentral area were non-damaged (Figure 10.8).



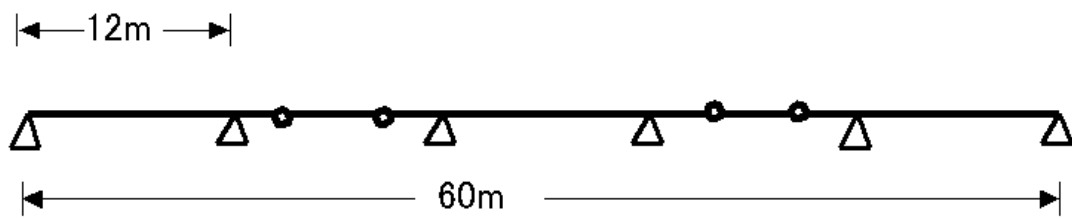
Figure 10.4: Non-damaged RC three-span highway bridge on Gayıt brook



Figure 10.5: Slightly-damaged RC three-span highway bridge on Çapakçur brook



(a) Göynük Brook Bridge on Bingöl-Muş Highway



(b) Structural mechanics model of Göynük Brook Bridge on Bingöl-Muş Highway



(c) Girder off-set of Gerber-type section of the bridge

Figure 10.6: A view, structural model and damaged section of Göynük Brook Bridge



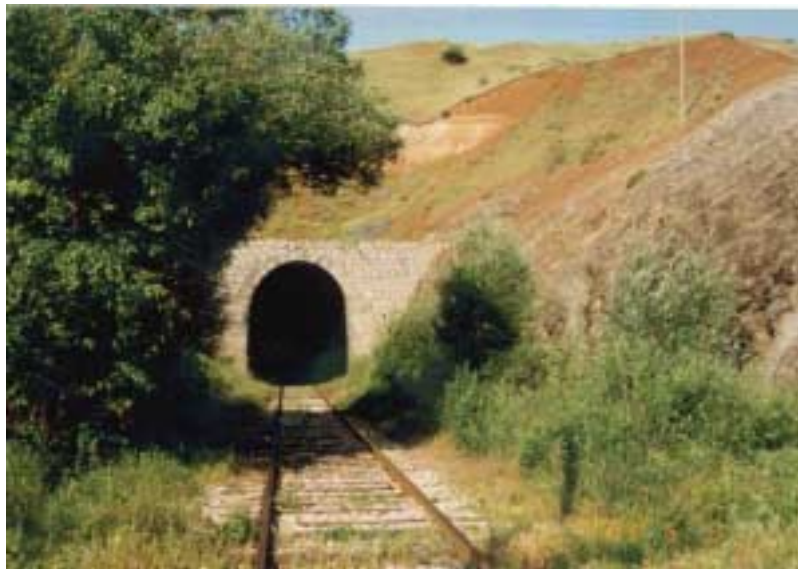
Figure 10.7: Non-damaged highway and railway bridges over Keban dam lake at Gülüşkür



Figure 10.8: Non-damaged bridges in the epicentral area

### 10.3 Tunnels

The tunnels in the earthquake region are associated with the state railway. There is no report about any damage to tunnels in the region. During the investigation, the authors could only check two tunnels. Figure 10.9 shows views of the single track tunnel at Gölüşkür and Palu. Palu is a town situated on the East Anatolian Fault and Murat River flow the town of Palu.



(a) Gölüşkür Tunnel nearby Keban Dam Lake



(b) Palu Tunnel along Murat River on East Anatolian Fault

Figure 10.9: Non-damaged railway tunnels at Gölüşkür and Palu

## 11 INDUSTRIAL AND STORAGE FACILITIES

The epicentral area is almost a non-industrialised region of Turkey. Since animal husbandry is the main economical income source of the region, industrial facilities are associated with the meat processing and storage. The damage at several important facilities is listed in Table 11.1.

Et-Kombinas owned by the state company (T.C. Et ve Balık Kurumu – Meat & Fish State Company) has a huge plant for animal slaughtering and meat processing and storage. The damage was limited to shear fracturing of some concrete columns. The building was a RC structure with solid brick infill walls. Since the machinery was fixed to the foundation through anchors, no sliding or overturning of machinery took place (Figure 11.1).

Binova Yem plant is an animal-food processing and storage facility. The RC structure is about 12m high and built in 1999 (Figure 11.2). Two columns of the building were heavily damaged. Nevertheless, no damage to machinery or silos of this plant was seen. The overturned fire-extinguisher device at this plant implied that the ground acceleration should have been greater 0.25g at this plant.

Yem Sanayii plant is owned by the state and it is mainly used for an animal-food storage facility. The plant has crushing and grinding units in an RC building built after the 1971 earthquake and steel storage silos, which are anchored to the foundation and connected to each other in a truss-type fashion (Figure 11.3). The visual inspection indicated that there was no structural damage to silos and RC building and machinery of the plant.

Turkish Roadway Authority (TCK) has a plant for crushing, paving and asphalt and gravel storage in Bingöl City. Asphalt is stored in vertical cylindrical tanks placed on concrete foundations and elevated horizontal cylindrical tanks (Figure 11.4). The inspections on vertical and horizontal tanks indicated that there was no earthquake-induced damage to the tanks. Crushed gravel is stored in a pre-cast storage-house. The pre-cast reinforced concrete panels were slightly displaced by the earthquake shaking. Nevertheless, the structure was structurally stable after the earthquake.

Table 11.1 Damage state of industrial and storage facilities in Bingöl Region

Factory or Plant Name	Damage State	Foundation (Location)
Et Kombinas	Structural damage to some columns. No damage to machinery. Machinery fixed to ground by anchors.	Soft Soil (Ekinyolu)
Binova Yem	Structural damage to columns. No damage to machinery and steel silos	Soft Soil (Ekinyolu)
Yem Sanayi	No structural damage to building or silos	Hard Terrace Soil (Bingöl Saray Mah.)
Turkish Roadway Authority (TCK)	No damage to storage tanks. Slight deformation of pre-cast panels of storage-house	Hard Terrace Soil (Bingöl Saray Mah.)



Figure 11.1: Some views of Et-kombinas plant



Figure 11.2: Views of Binova Yem Plant



Figure 11.3: Some views of Bingöl Yem Sanayi Plant



Figure 11.4: Some views of TCK plant

## 12 HYDRAULIC STRUCTURES

### 12.1 Dams

There are several dams around the earthquake epicenter and they are either earth-fill or rock-fill type built by DSI (Table 12.1 and Figure 12.1). The nearest dams to the earthquake epicenter are Gayt, Kiğı and Özlüce dams. While Gayt dam is an earthfill dam with rockblock facing for irrigation purpose built on Gayıt brook, Özlüce and Kiğı dams are rock-fill dams for hydraulic energy on Peri brook. The investigation team visited the site of Gayt dam, which was built on basaltic rock (Figure 12.2). While cracks at the crest of the dam was filled by the repair teams, no seepage was observed at the downstream side or any rotational failure towards the reservoir site, which is quite common form of failure for this type of dams. Nevertheless, a slight spreading type deformation on the upstream side towards the reservoir could be noticed as seen in Figure 12.2(a). No damage to spillways or gates were observed. There was a small earthfill dam nearby Gayt Dam as seen in Figure 12.2(e). Some small rotational movements were observed in the middle of dam nearby its crest on the downstream side. The movement was towards the epicenter.

Table 12.1: Dams nearby the earthquake epicenter

Dam Name	Height (m)	Type	Purpose	Distance to Epicenter (km)	Comment
Gayt	30.7	Earthfill	Irrigation	11.3	Axial cracks at crest
Gülbahar		Earthfill	Irrigation	22.5	No damage
Özlüce	144.0	Rockfill	Energy	32.5	No damage
Kiğı	144.0	Rockfill	Energy	32.5	No damage
Kalecik		Earthfill	Irrigation	33.8	No damage
Beyhanlı		Earthfill	Irrigation	40.0	No damage
Başköy		Earthfill	Irrigation	45.0	No damage
Kazan		Earthfill	Irrigation	50.0	No damage
Kaleköy		Earthfill	Irrigation	57.5	No damage
Keban	210	Rockfill	Energy	143.1	No damage
Karakaya	158.0	Gravity	Energy	136.2	No damage
Atatürk	169.0	Rockfill	Energy	241.3	No damage



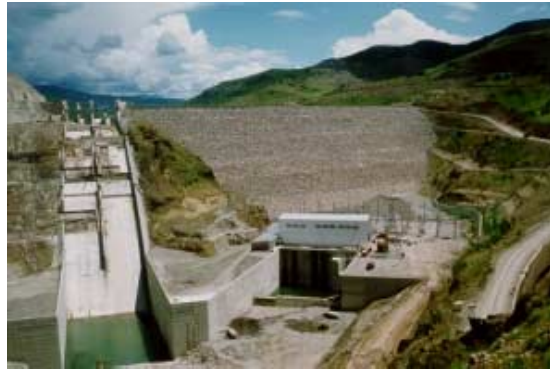
(a) Keban Dam



(b) Karakaya Dam



(c) Atatürk Dam



(d) Özlüce Dam



(e) Gayt Dam

Figure 12.1: Some views of major dams in the earthquake stricken region



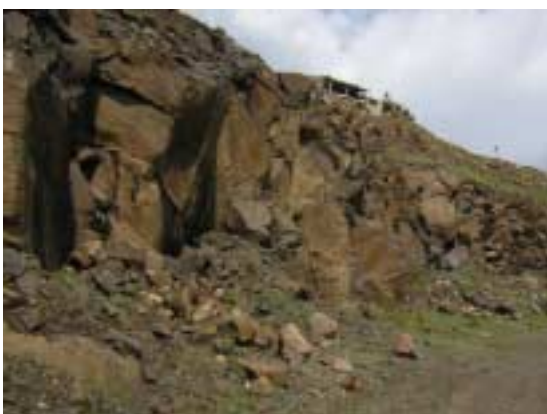
(a) Upstream side



(b) Spillways



(c) Repaired dam crest



(d) Foundation rock at RHS embankment



(e) A small earthfill dam nearby Gayt Dam

Figure 12.2: Some views of Gayt Dam

## 12.2 Channel Network

Bingöl basin is the largest basin in the province and it has an irrigation channel network for agricultural purposes. The channels have an inverted trapezoidal shape and were generally lined with lightly reinforced concrete panels (Figure 12.3). At two locations, the channels pass beneath Gayıt brook and Göynük brook through a siphon system. During the investigation no severe damage to the system was observed. Nevertheless, there was some slight seepage at the joints with the channel and concrete conduit type siphons, which indicated that some cracking took place. In spite of slight seepage from such spots, the system was functional.



Syphon system beneath Gayıt brook



Syphon system beneath Göynük brook



Figure 12.3: Some views of channels in Bingöl basin

### 13 DAMAGE TO STRUCTURES

The Crisis Center of Prime Ministry office declared the latest information as more than 176 casualty and 520 injury (as of May, 2003). The total number of collapsed or heavily damaged buildings is about 625. Buildings and structures built on alluvial deposits or nearby the crest of terraces mainly collapsed or heavily damaged while those founded on firm ground or rock were almost non-damaged.

In site investigations by the authors, it seems that reinforced concrete buildings suffered the most, particularly those having three or more stories founded on soft soils. Stone masonry buildings of single story were either slightly damaged or non-damaged if they were built in a traditional earthquake-proof style.

The main compound of mosques founded even on alluvial deposits experienced no-damage or slight damage while some of them lost their minarets. However, the collapse of minarets was few as compared with that at Çay-Eber earthquake (Ulusay et al. 2003). The main compounds of mosques were intact since they are structurally symmetric in accordance with the fundamental principles of earthquake-proof design since earlier times.

Table 13.1: The numbers of casualties injured people and damaged buildings in Bingöl City and towns and villages due to May 1, 2003 Earthquake

Location	Casualties	Injured	Collapsed-Heavily damaged	Moderately damaged	Lightly damaged	None damaged
Bingöl	60	370	362	493	989	1544
Çeltiksuyu	84	114				
Çimenli	13	10				
Göltepesi	2	4	3	11		
Sudüğünü	0	0	79	81	32	11
Arıcılar	0	0	9	8	38	17
Ekinyolu		-	87	3	121	58
Yazgülü			5	9	4	2
Kartal			11	7	18	35
Sancak			69	27	39	101
Haziran	1	1				
Ortancaçanak	2	15				
Çiriş	7	1				
Beyaztoprak	2	0				

### **13.1 Domes and Minarets**

Most of the main compounds of mosques in the earthquake affected region were intact or suffered very slight damage (Figures 13.1 and 13.2). The damage was generally concentrated at corners as observed in the previous earthquakes of Turkey. The main compounds of mosques generally have single dome or multiple semi-spherical domes and they are structurally symmetric. Probably for this reason, the main compounds remain intact during shaking. The main compounds of the mosques were damaged when the falling minarets hit the structures. The most severe damage was observed at Yeni Mahalle mosque in Bingöl due to also the weak-floor situation at its ground floor. The same type failures were also observed in the 1998 Adana-Ceyhan Earthquake and the 1999 Kocaeli and Düzce Earthquakes. Minarets in the region, which are generally 15 to 25 m high, are mainly non-reinforced cast-in place blocks. Minarets were mostly separated from the main compound of the mosques. Failures of minarets occurred at the junctions where the cross-section configuration of the structure changes from square to cylinder by toppling due to ground shaking (Aydan et al. 1999, Ulusay et al. 2003).



(a) Bingöl Yeni Mahalle Mosque (both minarets toppled)



(b) Bingöl Ulu Mosque



(c) Yolçatı Mosque

Figure 13.1: Damaged and non-damaged mosques

## 13.2 Damage to Buildings

### 13.2.1 Reinforced Concrete Structures

The totally collapsed or heavily damaged school, residential and office buildings had mainly 3-5 stories (Figure 13.3). These structures are designed as moment-resistant frame structures with in-fill walls made of hollow bricks. The diameter of reinforcing bars and stir-ups were mostly 13-16 mm and 3-4 mm, respectively. The bars were generally of smooth type. However, the use of deformed bars was observed in buildings under construction or new buildings. Most of heavily damaged or collapsed reinforced buildings were observed in Bingöl City, Ekinyolu, Çeltiksuyu, Kaleönü and Sarıçiçek villages. While Ekinyolu, Çeltiksuyu, Kaleönü and Sarıçiçek villages are located on soft alluvial deposits, Bingöl City was located over firm alluvial terrace deposits. The failure of RC structures was due to soft-story (weak-floor) situation as it is a common problem resulting in high casualties in earthquakes since 1960. The collapsed buildings were mostly located nearby the crest of terrace deposits bounded by three brooks, namely Gayıt, Çapakçur and Göynük (Figure 13.3). The ground floors of collapsed buildings were mostly used as either shops or garages. As a result, this type of usage constitutes a weak(soft)-floor situation. Furthermore, many buildings had heavy balconies of cantilever type.

The causes of damage were almost the same as those seen in the previous earthquakes of Turkey (Aydan and Hamada, 1992; Hamada and Aydan, 1992; Aydan and Kumsar 1997; Aydan et al., 1999; Ulusay et al., 2002). The causes listed below are taken from the reports by the first author on March 13, 1992 Erzincan Earthquake with few amendments and additions:

**Poor workmanship:** There are two kinds of poor workmanship. One of them is that the connections of columns and beams were very weak since the connections of steel bars were not properly done and detritus materials at such locations were not cleaned. The second one is that the granulometry of the sand and gravel of concrete was very poor and the range was wide. In addition, big chunks of gravel blocked the concrete during casting at locations where steel connections were dense and this resulted in very porous

and weak connections. Such connections were quite common in collapsed or heavily damaged buildings. During shaking, it seems that concrete at the connections first failed and this subsequently caused the buckling of steel bars at such locations and rupturing in-fill hollow brick walls in a brittle sense. As a result, the collapse of buildings ended up in a pancake mode.

**Construction negligence and lack of moral:** One of the most striking construction negligence was the confinement of concrete at the beam-column connections in spite of the Turkish design code for seismic regions. As stir-ups were very few at such locations, the failure of concrete was very brittle and it could not absorb the work done by the earthquake forces. Furthermore, the diameter of steel bars was less than that required which indicates the lack of moral of construction companies.

**Resonance:** Natural periods of collapsed buildings mostly coincided with those of the input waves and this resulted in the resonance-like shaking of structures and their subsequent collapses. For buildings having 3 to 5 stories, the natural period ranges between 0.15s and 0.25s. As explained through response analyses in Chapter 7, the collapse or severe damage of buildings on the basis of resonance phenomenon was mostly likely in Bingöl City.

**Soft Story:** Many buildings had shops at their ground floor. Since there are generally no shear-walls to take up the load during earthquakes, the total load is transferred onto the columns. The super structure acts as a top-heavy structure on the columns and in-fill walls, which are in poor contact with columns and beams, has no effect against the earthquake loading and they fail subsequently as seen in Figures 13.3 to 13.4). It was also interesting to note that structures having solid bricks or angular rock blocks as in-fill walls and columns constructed after the walls performed much better and damage was none or very limited. This good performance is probably due to the integrated behaviour of buildings during earthquake loading.

**Pounding of adjacent structures:** Buildings at the corners of streets were mostly collapsed as a result of pounding with the adjacent building.



(a) 3 story RC Primary school building at Çeltiksuyu



(b) 3 story RC Primary school building at Kaleönü



(c) Collapsed 4-5 story RC buildings

Figure 13.3: Views of collapsed RC buildings



(a) Soft-floor effect



(b) Column-beam joint



(c) Column-beam joints

Figure 3.14: Some examples of poor constructions

### 13.2.2 Stone Masonry Structures

The stone masonry buildings and stables are quite common particularly in villages. The wooden slabs of 9-10cm thick are installed at spacings of about 1m such that the integrity of the wall is achieved during construction and also the earthquakes (Figure 13.5). The walls are generally 60cm thick. The roofs are covered with thin corrugated zinc plates or earthen. Most severe damage was observed in houses with few wooden slabs and earthen heavy roofs. The houses made with appropriate spacing of wooden or concrete slabs for the continuity of structures performed very well during the earthquake.

Figure 13.5(b) shows a damaged one-story building. The damage to this buildings displayed some known characteristics of damage to masonry structures. Some walls fail by shearing and some walls fail by toppling (Aydan et al. 2003). The separation and damage occurred at the corners of the building in a well-known fashion. The difference in the behaviour of these two buildings may be directly related to the existence and continuity of slab-like elements within the structure. The damaged building has very short concrete slabs over the door and window openings and/or heavy roofs while the non-damaged building has all-around continuous concrete slabs with light roofs. Similar behaviors of stone masonry buildings were observed in other earthquakes such as the 1992 Erzincan, the 1995 Dinar, the 1998 Adana-Ceyhan and the 1999 Kocaeli Earthquakes, 2002 Çay-Eber earthquake (Hamada and Aydan, 1992; Aydan and Kumsar, 1997a; Aydan et al., 1998 and 1999a, Ulusay et al. 2002).



(a) Typical stone-masonry house



(b) The collapse of a stone masonry house (ground is very soft)



(c) Out-of plane failure



(d) Collapse of houses with heavy earthen roofs  
(note that standing houses have light roofs)

Figure 13.5: Views of damage to stone masonry houses

### 13.3 Water Towers

Water towers are RC structures and their height generally ranges between 25-30 meters. The towers generally have 6-8 columns and they are symmetric structures. Figure 13.6 shows two water towers together with a minaret at Saray district of Bingöl City. No damage was observed at these two water towers. The water tower in Çeltiksuyu village, where two RC 3-4 story buildings were collapsed, was not even slightly damaged (Figure 13.7). Taking into account observations in other Turkish earthquakes, the water towers exhibit a good performance during earthquakes. One reason is probably the period of this structure, while the other could be the damping effect of sloshing water in the water tanks.



Figure 13.6 Non-damaged water towers in Bingöl City nearby the strong-motion station



Figure 13.7: The non-damaged water tower in Çeltiksuyu village where two school buildings with 3-4 floors were all collapsed

## 14 CONCLUSIONS

In this report, the authors have described the site observations and information they have gathered during their investigation and made some preliminary assessments on different aspects of the May 1, 2003 Bingöl earthquake. The following conclusions are drawn from this study.

The Bingöl earthquake originated at a shallow depth ranging between 5 and 15 km according to several institutes and generated strong ground motion in Bingöl province and its close vicinity. Focal plane solutions from several institutes indicate two possible strike-slip faults striking NW-SE and NE-SW. However, site observations and distribution trend of the epicenters of the aftershock with  $M > 4.1$  suggest that the Sudüğünü fault, which has a right-lateral strike slip fault character and strikes in NW-SE direction, is the most probable causative fault when compared to other faults in the region. On the contrary to those observed in the devastating 1999 Kocaeli and Düzce earthquakes of Turkey, any evident surface rupture could not be traced on the land in this earthquake. Therefore, no structural damage associated with the surface rupture was encountered.

The maximum acceleration was recorded in NS direction as 545.5 gal at Bingöl station. Traces of acceleration response on horizontal plane indicated that initially the highest shaking magnitudes were in SE10 direction. This finding is consistent with the collapse and/or toppling directions of the structures measured by the authors in the earthquake region.

The acceleration spectra implied that buildings having three or more stories could have been subjected to very severe vertical shaking. Based on the acceleration spectra and natural periods of structures in Turkey, it can be concluded that buildings with 3-4 stories in Bingöl should be subjected to severe shaking.

The damages in Bingöl city center are concentrated nearby the cliffs of the terraces where inhabitation is relatively dense. This situation suggests a possible amplification at the cliff sides due to topographical effects. Based on the preliminary assessments from site observations and geotechnical borehole data, except topographical effects, it seems difficult to consider a relationship between local site conditions and damage to structures both on terraces and flat-lying areas in Bingöl and its close vicinity.

The landslides were generally concentrated close to epicenter of the earthquake. Heavy rains in the region within two weeks before the earthquake are considered to contribute to softening of the materials before they subjected to dynamic loads and made easy some failures to transform into mudflows.

The site observations indicated that reinforced concrete (RC) buildings suffered most, particularly those having three or more stories and school buildings. The main causes of heavy damage to RC buildings in this earthquake are generally similar to those in the previous earthquake.

- (a) Poor workmanship and poor granulometry of concrete,
- (b) Construction negligence and lack of moral,
- (c) Lack of implementation of seismic codes in structural design,
- (d) Soft story (weak floors),
- (e) Resonance-like phenomenon due to buildings natural periods and strong motion frequency characteristics.

The damage to transportation facilities, industrial facilities and lifelines was quite limited and it did not cause any severe functional disruption.

## ACKNOWLEDGEMENTS

The authors would like to sincerely express their thanks and gratitude to the following without their help this investigation could not be very fruitful within a very short period of time.

Japan Society of Civil Engineers (JSCE) financially supported the authors for visiting the earthquake region and to encourage publishing their findings and observations.

Turkish National Earthquake Committee and Turkish Earthquake Foundation, in particular Prof. Dr. Rifat Yarar, for his encouragement and his support to the investigation committee.

Research assistants Zeynal Abiddin Erguler, Nilsun Okan and Ergun Tuncay, and laboratory technician Ahmet Bay from the Geological Engineering Department of Hacettepe University, and Geological Engineer Elif Avşar for their kind help in editing the some parts of the manuscript, data assessment, and laboratory classification tests.

Hasan Ozaslan and M. Kemal Akman from Yüksel Project International Co., for providing borehole data for Bingöl and for their kind help for organization of the boring program at Hanoçayırı, and Münif Çelebi from the same company for his efficiency in performing the boring and for providing data.

Dr. Ömer Emre from the General Directorate of Mineral Research and Exploration of Turkey to share his information about the earthquake region with the authors.

The last, but not the least, the people of the earthquake stricken region are for their cooperation in gathering information on the extent of damage and guiding the authors to places of great significance (particularly, to Hilmi Aksoy from the Cadastral Survey of Bingöl, Kenan Birden from the Bingöl Municipality, Electrical Engineer Nusrettin Bartakuçin of TEDAŞ in Bingöl), kindness and generosity even though they suffered the most by losing their properties as well as their beloved ones.

## REFERENCES

- Aktan, H., Bayülke, N., Gül, A., Ergünay, O., Tabban, A., Yurdatapan, O., 1972. 22-5-1971 Bingöl Depremi, DAD-ERD, Ankara.
- Altınlı., E. 1963. Doğu ve Güneydoğu Anadolunun Jeolojisi. MTA Dergisi, 35-37.
- Aydan, Ö., 1997. The seismic characteristics and the occurrence pattern of Turkish earthquakes. Turkish Earthquake Foundation, Report No.: TDV/TR 97-007, 41p.
- Aydan, Ö., 2000. An stress inference method based on structural geological features for the full-stress components in the earth' crust, *Yerbilimleri*,22, 223-236.
- Aydan, Ö., 2001. İstanbul Boğazı denizaltı geçişi için tüp tünel ile kalkan tünelin uygunluğunun karşılaştırılması. *Jeoloji Mühendisliği*, 25(1), 1-17.
- Aydan, Ö. and M. Hamada, 1992. The site investigation of the Erzincan (Turkey) Earthquake of March 13, 1992. 4th Japan-US Workshop on earthquake Resistant Design of Lifeline Facilities and Countermeasures Against Soil Liquefaction, Honolulu, May, 17-34.
- Aydan, Ö. and Kumsar, H., 1995. A site investigation of Dinar earthquake of October 1, 1997. Turkish Earthquake Foundation, Report No. TDV/DR 97-003, 115p.
- Aydan, Ö., and Ulusay, R., 2002. Back analysis of a seismically induced highway embankment failure during the 1999 Düzce earthquake. *Environmental Geology*, 42(6), 621-631.
- Aydan, Ö., Sezaki, M., and Yarar, R., 1996. The seismic characteristics of Turkish Earthquakes. 11th World Conference on Earthquake Engineering, Acapulco, Mexico, CD-2, Paper No. 1025.
- Aydan, Ö., Ulusay, R., Kumsar, H., Sönmez, H., and Tuncay, E., 1998. A site investigation of Adana-Ceyhan earthquake of June 27, 1998. Turkish Earthquake Foundation, Report No. TDV/DR 006-30, 131p.
- Aydan, Ö., Ulusay, R., Haşgür, Z., and Taşkın, B., 1999. A site investigation of Kocaeli earthquake of August 17, 1999. Turkish Earthquake Foundation, TDV/DR 08-49, 180p.
- Aydan, Ö., Ulusay, R., Kumsar, H., and Tuncay, E., 2000. Site investigation and engineering evaluation of the Düzce-Bolu earthquake of November 12, 1999. Turkish Earthquake Foundation, Report No. TDV/DR 09-51, 307p.
- Aydan, Ö., Kumsar, H., and Ulusay, R., 2002. How to infer the possible mechanism and characteristics of from the striations and ground surface traces of existing faults. *JSCE, Earthquake and Structural Engineering Division I, Special Issue*, 19(2), 199-208.
- Barka, A.A. and K. Kadinsky-Cade, 1988. Strike-slip fault geometry in Turkey and its influence on earthquake activity, *Tectonics*, 7, pp.663-684.
- DAD/ERD, 2003. <http://www.deprem.gov.tr> (May, 2003).
- Emre, Ö., Herece, E., Doğan, A., Parlak, O., Özaksoy, V., Cıplak, R ve Özalp, S., 2003. 1 Mayıs 2003 Bingöl Depremi. <http://www.mta.gov.tr/Bingol/Bingol.asp>, 17s (unpublished report).
- ERI, 2003. <http://www.eri.u-tokyo.ac.jp/> (May, 2003).

- Ergin, K., Güçlü, U. and Uz, Z., 1967. Türkiye ve civarının deprem kataloğu (The catalogue of earthquakes of Turkey), İTÜ, Yer Fiziği Enstitüsü, Yayın No. 24, İstanbul.
- Eyidoğan, H., U. Güçlü and Z. Utku, E. Değirmenci 1991. Türkiye büyük depremleri makro-sismik rehberi, İTÜ.
- Hamada, M., and Aydan, Ö., 1992. The site investigation of the March 13, 1992 earthquake of Erzincan, Turkey. ADEP, Association for Development of Earthquake Prediction, 86p.
- HARVARD, 2003. <http://www.eic.eri.u-tokyo.ac.jp/~cmt/HARVARD/> (May, 2003).
- Hamada, M., Yasuda, S., Isoyama, R., and Emoto, K., 1986. Study on liquefaction induced permanent ground displacements. Report for the Japan Association for the Development of Earthquake Prediction.
- Gülen, L., Pınar, A., Kalafat, D., Özel, N., Horasan, G., Yılmaz, M., and Işıkara, A.M., 2002, Surface faults breaks aftershock distribution, and rupture process of the 17 August 1999 İzmit, Turkey, earthquake. Bull. Seism. Soc. Amer., 92 (1), 230-244.
- Ketin, İ. 1973. Umumi Jeoloji (General Geology). *Published by İ. T. Ü.*, No: 30. İstanbul.
- KOERI, 2003. <http://www.koeri.boun.edu.tr> .
- Japan Port Harbor Research Institute, 1997. Handbook on Liquefaction Remediation of Reclaimed Land. A.A. Balkema, Rotterdam, 312 p.
- Midorikawa, S., 1987. Prediction of isoseismal map in the Kanto Plain due to hypothetical earthquake. Journal of Structural Engineering, 33B, 43-48.
- Ohba, S., and Trauma, I., 1970. Dynamic response characteristics of Osaka Plain. Proc. Annual Meeting A.I.J. (In Japanese).
- Şaroğlu, F., Emre, Ö., Kuşçu, İ. (1992): The east Anatolian fault zone of Turkey, *Annales Tectonicae*, Special Issue-Supplement to Volume VI, 99-125.
- Şengör, A.M.C., 1979. The North Anatolian transform fault: its age, offset and tectonic significance, J. Geol. Soc. London, 136, pp. 269-282.
- Seymen, İ. and Aydın, A., 1972. Bingöl deprem fay ve bunun Kuzey Anadolu Fay Zonu ile ilişkisi. MTA Dergisi, 79, 1-8.
- Technical Committee for Earthquake Geotechnical Engineering, 1999. Manual for Zonation on Seismic Hazards. Revised Version, Publication of the Japanese Geotechnical Society, 209 p.
- TÜBİTAK-MAM, 2003. <http://www.mam.gov.tr/> .
- Ulusay, R., Aydan, Ö., Kumsar, H., and Sönmez, H., 2000. Engineering geological characteristics of the 1998 Adana-Ceyhan earthquake with particular emphasis on the liquefaction phenomenon and the role of soil behaviour. Bulletin Engineering Geology and the Environment, 59(2), 99-118.
- USGS-NEIC (2003): <http://neic.usgs.gov/>.
- Youd, T.L., Idriss, I.M., Andrus, R.D., Arango, I., Castro, G., Christian, J.T., Dobry, R., Finn, W.D.L., Harder, L.E., Hynes, M.E., Ishihara, K., Koester, J.P., Liao, S.S.C., Marcuson, W.F., Martin, G.R., Mitchell, J.K., Moriwaki, Y., Power, M.S., Robertson, P.K., Seed, R.B., and Stokoe, K.H., 2001. Liquefaction resistance of soils: Summary report from the 1996 NCEER/NSE workshops on evaluation of liquefaction resistance of soils. J. Geotechnical and Geoenvironmental Engineering ASCE, 127(4), 817-833.
- Yüksel Proje A.Ş., 2003a. Bingöl kalıcı deprem konutları jeolojik-jeoteknik etüt raporu. 26 p (unpublished report).

- Yüksel Proje A.Ş., 2003b. Bingöl kenti sondajlarına ait sondaj logları (unpublished borehole logs).
- Yüksel Proje A.Ş., 2003c. Çeltiksuyu Yatılı İlköğretim Okulu jeolojik-jeoteknik etüt raporu. 28 p (unpublished report).